Title

Epithermal mineralization controlled by synextensional magmatism in the Guazapares Mining District of the Sierra Madre Occidental silicic large igneous province, Mexico

Authors

Murray, Bryan P

Busby, Cathy J

Publication Date

2015-03-01

DOI

10.1016/j.jsames.2014.12.009

Peer reviewed

Journal of South American Earth Sciences 58 (2015) 1–18

Contents lists available at ScienceDirect

Journal of South American Earth Sciences

journal homepage: www.elsevier.com/locate/jsames

Epithermal mineralization controlled by synextensional magmatism in the Guazapares Mining District of the Sierra Madre Occidental silicic large igneous province, Mexico

Bryan P. Murray*, Cathy J. Busby

Department of Earth Science, University of California, Santa Barbara, Webb Hall, Santa Barbara, CA 93106-9630, USA

ARTICLE INFO

Article history:
Received 13 July 2014
Accepted 29 December 2014
Available online 8 January 2015

Keywords:
Epithermal mineralization
Extension
Silicic large igneous province
Sierra Madre Occidental
Mexico
Ignimbrite flare-up

ABSTRACT

We show here that epithermal mineralization in the Guazapares Mining District is closely related to extensional deformation and magmatism during the mid-Cenozoic ignimbrite flare-up of the Sierra Madre Occidental silicic large igneous province, Mexico. Three Late Oligocene–Early Miocene syn-extensional formations are identified by detailed volcanic lithofacies mapping in the study area: (1) ca. 27.5 Ma Parajes formation, composed of silicic outflow ignimbrite sheets; (2) ca. 27–24.5 Ma Témoris formation, consisting primarily of locally erupted mafic-intermediate composition lavas and interbedded fluvial and debris flow deposits; (3) ca. 24.5–23 Ma Sierra Guazapares formation, composed of silicic vent to proximal ignimbrites, lavas, subvolcanic intrusions, and volcaniclastic deposits. Epithermal low- to intermediate-sulfidation, gold–silver–lead–zinc vein and breccia mineralization appears to be associated with emplacement of Sierra Guazapares formation rhyolite plugs and is favored where pre-to-synvolcanic extensional structures are in close association with these hypabyssal intrusions.

Several resource areas in the Guazapares Mining District are located along the easternmost strands of the Guazapares Fault Zone, a NNW-trending normal fault system that hosts most of the epithermal mineralization in the mining district. This study describes the geology that underlies three of these areas, which are, from north to south: (1) The Monte Cristo resource area, which is underlain primarily by Sierra Guazapares formation rhyolite dome collapse breccia, lapilli-tuffs, and fluvially reworked tuffs that interfinger with lacustrine sedimentary rocks in a synvolcanic half-graben bounded by the Sangre de Cristo Fault. Deposition in the hanging wall of this half-graben was concurrent with the development of a rhyolite lava dome-hypabyssal intrusion complex in the footwall; mineralization is concentrated in the high-silica rhyolite intrusions in the footwall and along the syndepositional fault and adjacent hanging wall graben fill. (2) The San Antonio resource area, underlain by interstratified mafic-intermediate lavas and fluvial sandstone of the Témoris formation, faulted and tilted by two en echelon NW-trending normal faults with opposing dip-directions. Mineralization occurs along subvertical structures in the accommodation zone between these faults. There are no silicic intrusions at the surface within the San Antonio resource area, but they outcrop ~0.5 km to the east, where they are intruded along the La Palmera Fault, and are located ~120 m-depth in the subsurface. (3) The La Unión resource area, which is underlain by mineralized andesite lavas and lapilli-tuffs of the Témoris Formation. Adjacent to the La Unión resource area is Cerro Salitrera, one of the largest silicic intrusions in the area. The plug that forms Cerro Salitrera was intruded along the La Palmera Fault, and was not recognized as an intrusion prior to our work.

We show here that epithermal mineralization is Late Oligocene to Miocene-age and hosted in extensional structures, younger than Laramide (Cretaceous-Eocene) ages of mineralization inferred from unpublished mining reports for the region. We further infer that mineralization was directly related to the emplacement of silicic intrusions of the Sierra Guazapares formation, when the mid-Cenozoic ignimbrite flare-up of the Sierra Madre Occidental swept westward into the study area about 24.5–23 Ma ago.

* Corresponding author.
E-mail address: bmurray@umail.ucsb.edu (B.P. Murray).

http://dx.doi.org/10.1016/j.jsames.2014.12.009
0895-9811/

1. Introduction

The Sierra Madre Occidental of northwestern Mexico is the largest Cenozoic silicic igneous province on Earth (300,000–400,000 km^3; Aguirre-Díaz and Labarthe-Hernández, 2003; Bryan, 2007; Ferrari et al., 2007; Bryan and Ferrari, 2013). The Sierra Madre Occidental also hosts one of the largest (800,000 km^2) and most productive (at least 80 million ounces gold, 4.5 billion ounces silver produced) epithermal precious mineral belt on Earth (Dreier, 1984; Staude and Barton, 2001). As important as these mineral deposits are, there is a limited understanding of the relationships between the timing of epithermal mineralization and the magmatic and tectonic history of the Sierra Madre Occidental, particularly at mining district levels. Regional tectonic controls on the development of epithermal veins in western North America have been proposed (e.g., Dreier, 1984; Price et al., 1988), and Staude and Barton (2001) suggested that Jurassic to Late Cenozoic mineralization is commonly associated with coeval magmatic and tectonic events. In the case of Mexican epithermal deposits, Camprubí et al. (2003) suggest that the age of the volcanic host rock is close to the age of the mineralization. However, the details of the structural setting of the precious mineral deposits, and their relationship to specific magmatic and tectonic events, remain poorly known for most of the Sierra Madre Occidental.

The Guazapares Mining District of western Chihuahua, Mexico is located ~250 km southwest of Chihuahua City in the northern part of the Sierra Madre Occidental (Fig. 1), within the Sierra Madre Occidental Gold–Silver Belt. Previous work in the Guazapares Mining District is restricted to unpublished mining company reports, except for our recently published work (Murray et al., 2013). These unpublished reports (e.g., Roy et al., 2008; Wood and Durgin, 2009; Gustin, 2011, 2012) indicate that mineralization in the Guazapares Mining District is spatially associated with the north-

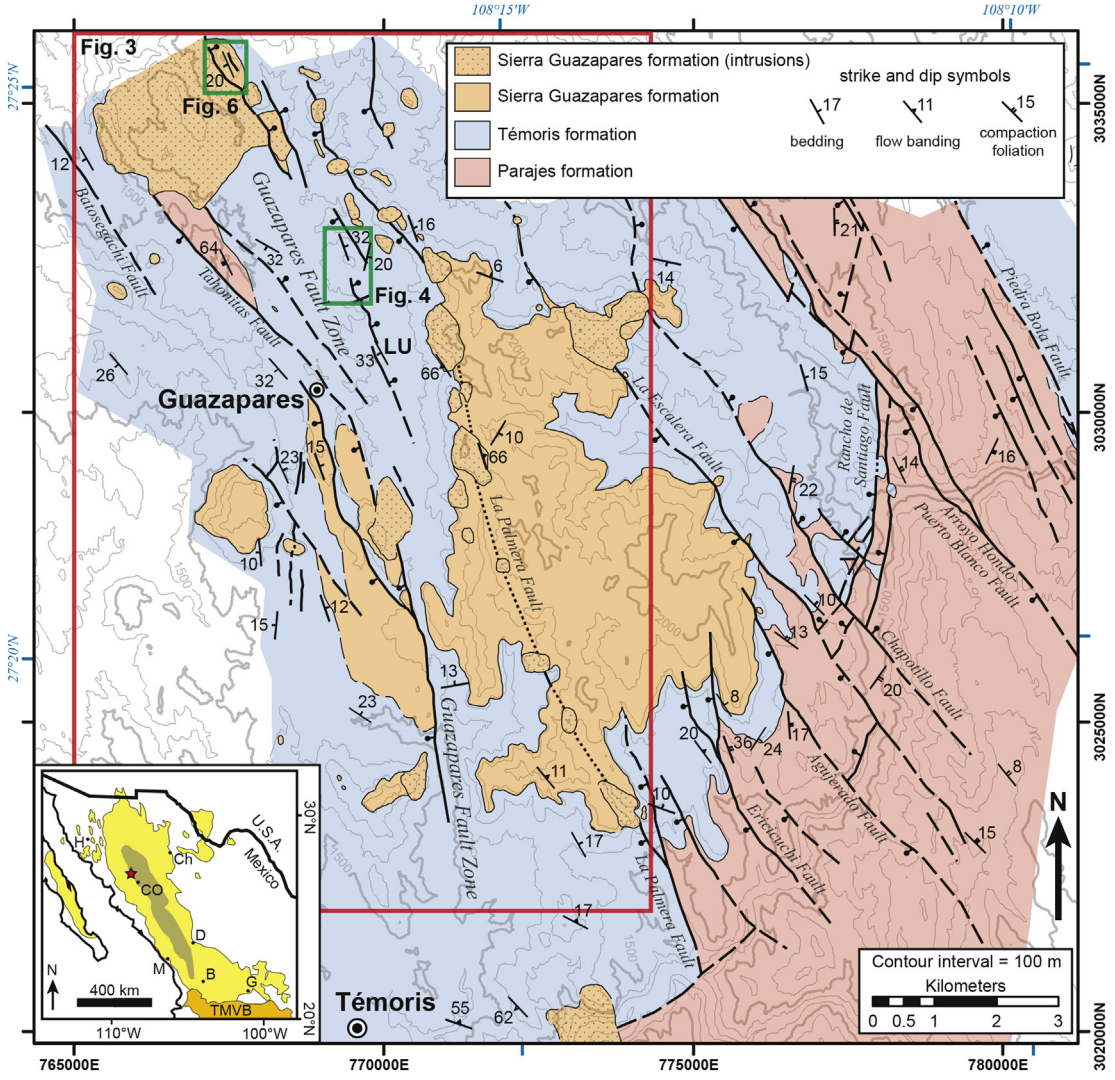

Fig. 1. Simplified geologic map of the Guazapares Mining District region, showing the extent of the three formations (Fig. 2) and the location of major faults (after Murray et al., 2013). The Guazapares Mining District lies north of the town of Témoris, which is a stop on the famous Copper Canyon train. The red box indicates the location of Fig. 3 (shown on two pages below), which focuses on the Guazapares Fault Zone; for detailed discussion of the entire map area, see Murray et al. (2013). The green boxes indicate the locations of the San Antonio (Fig. 4) and Monte Cristo (Fig. 6) resource areas; LU—La Unión resource area. Inset map of western Mexico shows the extent of the Sierra Madre Occidental (SMO) silicic large igneous province (light yellow) and the relatively unextended core (dark gray) of the SMO (after Henry and Aranda-Gómez, 2000; Ferrari et al., 2002; Bryan et al., 2013). The star indicates the location of the Guazapares Mining District (this study). B—San Martín de Bolaños Mining District, CO—Cuenca de Oro basin, Ch—Ciudad Chihuahua, D—Durango, G—Guanajuato Mining District, H—Hermosillo, M—Mazatlán, TMVB—Trans-Mexican Volcanic Belt. (For interpretation of the references to color in this figure legend, the reader is referred to the web version of this article.)

northwest trending, steeply dipping structures of the Guazapares Fault Zone and consists of multi-phase, epithermal, low-to-intermediate-sulfidation, gold–silver–lead–zinc vein and breccia deposits. These studies focus mainly on the alteration and mineralization zones within the mining district, and less on the physical volcanology and structure of the host rocks. Here, we assess the mining district in the context of the broader geologic setting and regional volcanotectonic evolution, by mapping volcanic and intrusive lithofacies and their relationships with faults, with additional petrographic, geochemical, and geochronological data on the igneous rocks. The approach described above has been previously employed to reconstruct the volcanic and tectonic history of the Guazapares Mining District region (Murray et al., 2013). In this study, we describe the broader magmatic and tectonic controls on epithermal mineralization in the Guazapares Mining District and present new interpretations based on detailed volcanic lithofacies mapping in the locations of active mining prospects within the Guazapares Mining District to interpret the magmatic and structural setting of these mineral deposits. We propose that epithermal mineralization is favored where pre-to-synvolcanic extensional structures were reactivated or became active during emplacement of rhyolite hypabyssal intrusions of the silicic large igneous province, and that the timing of mineralization is synchronous with emplacement of these intrusions.

2. Geologic background

The Sierra Madre Occidental silicic large igneous province is considered part of the extensive mid-Cenozoic ignimbrite flare-up that affected much of the southwestern North American Cordillera from the Middle Eocene to Late Miocene (e.g., Coney, 1978; Armstrong and Ward, 1991; Ward, 1991; Ferrari et al., 2002; Lipman, 2007; Cather et al., 2009; Henry et al., 2010; Best et al., 2013). The Sierra Madre Occidental trends for ~1200 km southwest from the U.S.–Mexico border to the Trans-Mexican Volcanic Belt (Fig. 1), consisting primarily of Oligocene to Early Miocene ignimbrites that cover an area of ~400,000 km^2 with an average thickness of 1 km (McDowell and Keizer, 1977; McDowell and Clabaugh, 1979; Aguirre-Díaz and Labarthe-Hernández, 2003; Bryan and Ferrari, 2013). The core of the Sierra Madre Occidental is relatively unextended in comparison to the surrounding Late Oligocene-to Miocene-age extensional belts of the southern Basin and Range to the east and the Gulf Extensional Province to the west (Fig. 1; Nieto-Samaniego et al., 1999; Henry and Aranda-Gómez, 2000; Ferrari et al., 2013).

2.1. Regional volcanic stratigraphy

Previous regional studies have subdivided the Late Cretaceous to mid-Cenozoic rocks of the Sierra Madre Occidental into: (1) the Late Cretaceous to Eocene Lower Volcanic Complex, (2) the Eocene to Early Miocene Upper Volcanic Supergroup, and (3) the Early Oligocene to Early Miocene Southern Cordillera basaltic andesite (SCORBA) (McDowell and Keizer, 1977; Cameron et al., 1989; Ferrari et al., 2007). The Lower Volcanic Complex is dominantly intermediate in composition and is interpreted as continental subduction-related magmatism broadly contemporaneous with the Laramide orogeny in western North America (McDowell and Keizer, 1977; McDowell et al., 2001; Staude and Barton, 2001). The Lower Volcanic Complex is inferred to underlie most of the Upper Volcanic Supergroup (Aguirre-Díaz and McDowell, 1991; Ferrari et al., 2007), which is composed mainly of silicic ignimbrites, lavas, and intrusions (McDowell and Keizer, 1977; McDowell and Clabaugh, 1979; Aguirre-Díaz and McDowell, 1991, 1993; Ferrari et al., 2002, 2007; McDowell, 2007). The rocks of the Upper Volcanic Supergroup represent the products of episodic large-volume silicic large igneous province magmatism during the mid-Cenozoic ignimbrite flare-up that affected much of the southwestern North American Cordillera from the Middle Eocene to Late Miocene (e.g., McDowell and Keizer, 1977; Ferrari et al., 2007; Lipman, 2007; Cather et al., 2009; Henry et al., 2010; Best et al., 2013), with major ignimbrite eruptive pulses during the Eocene (ca. 46–42 Ma), Early Oligocene (ca. 32–28 Ma), and Early Miocene (ca. 24–20 Ma) (Ferrari et al., 2002, 2007; Cather et al., 2009; McDowell and McIntosh, 2012). During the final stages of, and after each ignimbrite pulse of the Upper Volcanic Supergroup, mafic to intermediate composition lavas referred to as Southern Cordillera basaltic andesite (SCORBA) were intermittently erupted in the northern Sierra Madre Occidental (e.g., Cameron et al., 1989; Cochemé and Demant, 1991; Gans, 1997; McDowell et al., 1997; González-León et al., 2000; Ferrari et al., 2007).

The transition from intermediate arc magmatism (Lower Volcanic Complex) to silicic and mafic-intermediate magmatism (Upper Volcanic Supergroup and SCORBA) is interpreted as the result of decreased convergence between the Farallon and North American plates beginning in the Late Eocene ca. 40 Ma (Wark et al., 1990; Aguirre-Díaz and McDowell, 1991; Ward, 1991; Wark, 1991; Grijalva-Noriega and Roldán-Quintana, 1998; Ferrari et al., 2007). After the end of the Laramide orogeny in Mexico (Late Eocene), the Farallon plate is interpreted to have been removed from the base of the North American plate, likely by slab rollback (e.g., Ferrari et al., 2007; Henry et al., 2010; Best et al., 2013; Busby, 2013) or through the development of a slab window (e.g., Dickinson and Snyder, 1979; Wong et al., 2010). Removal of the slab resulted in a general southwestward migration of the arc-front magmatism towards the trench, commencing by ca. 40 Ma, in response to these Farallon–North American plate interactions (e.g., Coney and Reynolds, 1977; Damon et al., 1981; Ferrari et al., 1999, 2007; Gans et al., 2003; Henry et al., 2010; Busby, 2012; McDowell and McIntosh, 2012; Bryan et al., 2013; Busby, 2013).

2.2. Timing of crustal extension

The timing of crustal extension in the northern Sierra Madre Occidental in relation to silicic ignimbrite flare-up volcanism is poorly constrained. Previous workers have suggested that significant crustal extension in the Sierra Madre Occidental did not occur until after the Early Oligocene peak of Upper Volcanic Supergroup volcanism (e.g., McDowell and Clabaugh, 1979; Cameron et al., 1989; Wark et al., 1990; McDowell and Mauger, 1994; Gans, 1997; McDowell et al., 1997; Grijalva-Noriega and Roldán-Quintana, 1998) and that SCORBA magmatism records the initiation of regional crustal extension following this ignimbrite pulse (e.g., Cameron et al., 1989; Cochemé and Demant, 1991; Gans, 1997; McDowell et al., 1997; González-León et al., 2000; Ferrari et al., 2007). Alternatively, other studies have inferred that either the onset of large volume Early Oligocene ignimbrite flare-up volcanism records initial regional extension (e.g., Aguirre-Díaz and McDowell, 1993), or that extension may have began as early as the Eocene, based on the orientation and age of epithermal vein deposits (Dreier, 1984) and a moderate angular unconformity between the Lower Volcanic Complex and Upper Volcanic Supergroup (e.g., Ferrari et al., 2007). In this paper, we summarize evidence, described in detail by Murray et al. (2013), that extension in the Guazapares Mining District began during the Early Oligocene ignimbrite pulse (ca. 32–28 Ma), which occurred to the east of the study area, and continued through the Early Miocene ignimbrite pulse (ca. 24–20 Ma), which occurred within the Guazapares Mining District.

2.3. Timing of epithermal mineralization

As noted above, metallic mineralization is widespread in northwestern Mexico, and has been inferred to be broadly coeval with regional Late Jurassic to Late Cenozoic magmatic events (e.g., Staude and Barton, 2001; Camprubí et al., 2003). The majority of low-sulfidation epithermal deposits in Mexico range from Eocene to Miocene age (Albinson et al., 2001; Camprubí et al., 2003). Based on the assumption that the age of the volcanic host rocks is an approximation of the age of epithermal mineral deposits, and supported by limited direct dating of adularia from mineral deposits, Camprubí et al. (2003) proposed that there are three main phases of epithermal mineralization in the Sierra Madre Occidental: (1) a first phase between ca. 48 and 40 Ma, related to Laramide magmatism; (2) a second phase between ca. 40 and 27 Ma, related to the Early Oligocene pulse of the ignimbrite flare-up; and (3) a third phase between ca. 23 and 18 Ma, related to the Early Miocene pulse of the ignimbrite flare-up (Camprubí et al., 2003). Laramide-age mineralization is hosted by rocks of the Lower Volcanic Complex, generally in E–W trending veins oriented perpendicular to the least compressional stress direction (Dreier, 1984; Price et al., 1988; Camprubí et al., 2003). Many of these epithermal deposits are likely buried beneath the ignimbrite sheets of the Upper Volcanic Supergroup (Staude and Barton, 2001). It has been inferred that the majority of epithermal deposits in Mexico formed during Upper Volcanic Supergroup magmatism, which created a NW-trending mineralized belt from Guerrero to Chihuahua, at a distance of up to ~250 km from the Pacific coast (Camprubí et al., 2003). NW–SE trending of the epithermal veins of this age are generally interpreted to be normal to the direction of maximum regional extension (e.g., Dreier, 1984; Price et al., 1988). Mineral deposits hosted in the Upper Volcanic Supergroup have been widely assumed to be related to the Early Oligocene ignimbrite pulse, because the Early Miocene pulse was not widely recognized (Camprubí et al., 2003), except for recent studies in the southern Sierra Madre Occidental (Ferrari et al., 2002, 2013). However, for the most part, the mineralization lacks precise age control because the host rocks in most of the Sierra Madre Occidental are very poorly mapped and dated.

2.4. Volcanic terminology

The use of volcanic-volcaniclastic terminology in the literature is often ambiguous. The terminology we use in this paper are those of Fisher and Schmincke (1984), Fisher and Smith (1991), Sigurdsson et al. (2000), and Jerram and Petford (2011). Three main types of volcanic rocks are found in the Guazapares Mining District: extrusive (e.g., lavas, domes), hypabyssal (e.g., plugs), and volcaniclastic. Following Fisher and Schmincke (1984), volcaniclastic refers to all fragmental rocks made dominantly of volcanic detritus: these include (1) pyroclastic fragmental deposits, inferred to have been directly fed from an eruption, e.g., pyroclastic fall, ignimbrites, pyroclastic surges, dome-collapse breccias, block-and-ash flows, autoclastic flow breccias; (2) reworked fragmental deposits, inferred to result from downslope reworking of unconsolidated eruption-fed fragmental deposits, e.g., block-and-ash flow deposits commonly pass downslope into debris flow and fluvial deposits, and delicate pyroclastic detritus (pumice, shards, or euhedral crystals) indicate limited transportation of unconsolidated primary volcanic material; and (3) epiclastic deposits, made of volcanic fragments inferred to have been derived from erosion of preexisting rock. When the distinctions cannot be made, the general term volcaniclastic is applied.

3. Geology of the Guazapares Mining District

3.1. Lithology and depositional setting

The rock types and depositional setting of the Guazapares Mining District region are briefly summarized below to provide a stratigraphic and tectonic framework; further detailed descriptions of these deposits and the history of volcanic and tectonic development are provided by Murray et al. (2013).

Three informal formations are recognized in the Guazapares Mining District region (Figs. 1 and 2), consisting of: (1) silicic outflow ignimbrites of the Parajes formation, (2) mafic to andesitic volcanic rocks and intrusions of the Témoris formation; and (3) vent-related silicic ignimbrites, lavas, and plugs of the Sierra Guazapares formation. These rocks record Late Oligocene to Early Miocene (Upper Volcanic Supergroup) synextensional deposition and magmatism during the mid-Cenozoic ignimbrite flare-up (Murray et al., 2013). Older regional geologic maps (e.g., Minjárez-Sosa et al., 2002; Ramírez-Tello and García-Peralta, 2004) and recent mining company reports (e.g., Roy et al., 2008; Wood and Durgin, 2009; Gustin, 2011, 2012) in the Guazapares Mining District have widely referred to the andesitic rocks that underlie ridge-capping silicic volcanic rocks as “Lower Volcanic Complex”, but our new mapping and geochronology over a broader region (Figs. 2 and 3) shows that those andesitic rocks (Témoris formation) are sandwiched between silicic volcanic rocks (Parajes and Sierra Guazapares formations). Thus, the andesitic rocks in the Guazapares Mining District are not Eocene rocks with Laramide-related orogenic structures; instead, they record local development of a ca. 27–24.5 Ma andesitic center in the Upper Volcanic Supergroup, under an extensional strain regime (Murray et al., 2013), as summarized below.

The Parajes formation is composed of welded to nonwelded silicic outflow ignimbrite sheets, with lesser locally interbedded sandstone, conglomerate, and reworked tuff derived from erosion of these ignimbrites. These rocks mainly outcrop to the northeast of Témoris (Fig. 1), where they clearly underlie the Témoris formation and lie within extensional basins (Murray et al., 2013). The silicic outflow ignimbrite sheets were erupted ca. 27.5 Ma (Fig. 2), during the end of the Early Oligocene pulse of the mid-Cenozoic ignimbrite flare-up. The source of these ignimbrites is likely calderas of similar age that lie mainly 50–100 km to the east of the study area (Murray et al., 2013).

The Témoris formation records local mafic to intermediate composition magmatism and distal silicic ignimbrite volcanism, as well as sedimentation in graben-filling alluvial fan systems, with ages between ca. 27 and 24.5 Ma (Fig. 2). The Témoris formation is subdivided into three sections with gradational contacts (Fig. 2), composed of: (1) a lower section of amygdaloidal basalt, basaltic andesite, and andesite intrusions, lavas and autoclastic flow breccias, with locally interbedded silicic tuff in the lowermost deposits; (2) a middle section of andesite intrusions and flow-banded andesite lavas; and (3) an upper section of distal thin nonwelded rhyolite ignimbrites and tuffaceous volcaniclastic deposits (reworked and epiclastic) (Murray et al., 2013). Volcaniclastic debris flow breccias and fluvial conglomerates and sandstones are interbedded with all of the volcanic rocks listed above; these deposits contain detritus similar in composition to the interstratified volcanic rocks, suggesting resedimentation of primary eruptive products. The lavas and associated subvolcanic intrusions of the lower and middle sections of the Témoris formation form an andesitic center sited in the area around Témoris (Fig. 3), but lavas were also likely fed from fault-controlled dikes that lie outside this main center. The distal ignimbrites and sedimentary rocks of the upper section of the Témoris formation record a local eruptive

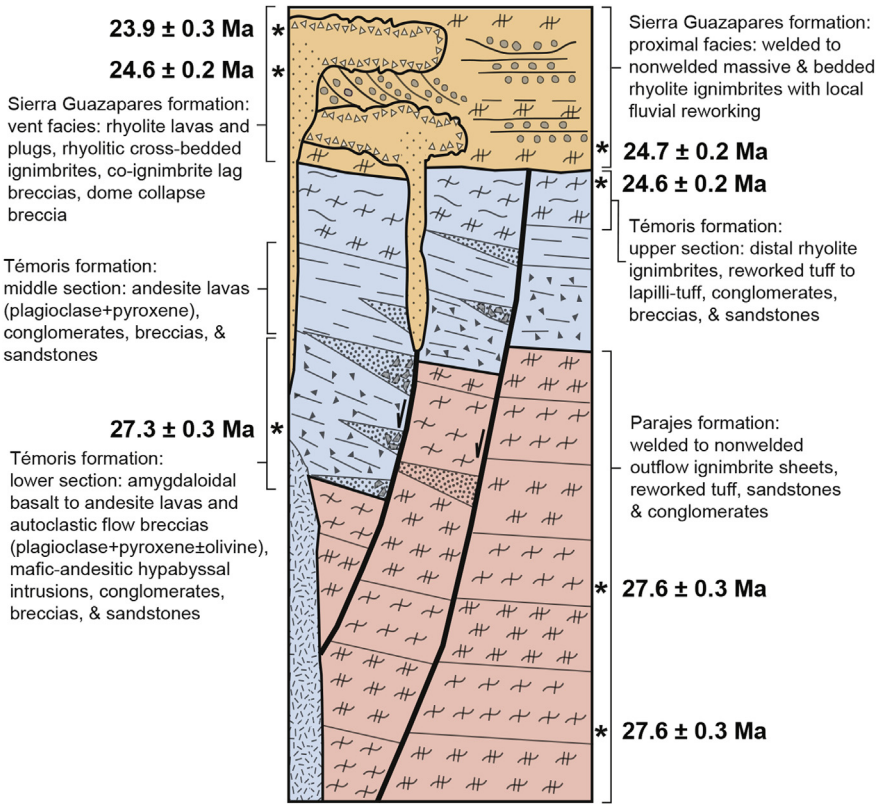

Fig. 2. Generalized stratigraphic column of the Guazapares Mining District region, depicting the characteristics and depositional relationships between the Parajes formation, Témoris formation, and the Sierra Guazapares formation (after Murray et al., 2013). Age data are from zircon U–Pb laser ablation ICP-MS geochronology by Murray et al. (2013).

hiatus between mafic-andesitic magmatism of the Témoris Formation and silicic magmatism of the Sierra Guazapares formation. The rocks of the Témoris formation have experienced mild to intense alteration, including hematitic and propylitic, and the infilling of vesicles and autoclastic flow breccia interstices with zeolite minerals (Murray et al., 2013). In addition, the Témoris Formation hosts most of the epithermal precious metal mineralization along the Guazapares Fault Zone (e.g., Roy et al., 2008; Wood and Durgin, 2009; Gustin, 2011, 2012), including the San Antonio and La Unión resource areas, described below.

The Sierra Guazapares formation records the local emplacement of silicic volcanic and hypabyssal rocks from fault-controlled fissure vents across a region that includes the Guazapares Mining District, with ages between ca. 24.5 and 23 Ma (Fig. 2), at the onset of the Early Miocene pulse of the mid-Cenozoic ignimbrite flare-up. Vent to proximal volcanic rocks of this formation crop out in an 11-km long and 3 km-wide linear belt along the La Palmera Fault–Guazapares Fault Zone (Fig. 3). These include rhyolitic ignimbrites with lithic lag breccias and very large-scale cross bedding that laterally transition away from this linear belt into massive to stratified ignimbrites. Rhyolite plugs, some of which pass continuously upward into rhyolite lavas that overlie the ignimbrites, also outcrop in this linear belt, as well as along other faults within the study area (Figs. 1 and 3). The Sierra Guazapares formation is generally less altered than the underlying Témoris formation (Murray et al., 2013); however, altered rocks in the Monte Cristo resource area, described in detail below, belong to the linear belt of Sierra Guazapares formation silicic vent facies rocks and intrusions along the La Palmera Fault–Guazapares Fault Zone.

The main geologic structures in the Guazapares Mining District region are NNW-trending normal faults, including the Guazapares Fault Zone and faults to the northeast of Témoris (Figs. 1 and 3). Several normal faults located northeast of Témoris (Fig. 1) bound half-graben basins and have significant displacement, with ~100 to >450 m vertical offset and at least 20% total horizontal extension (Murray et al., 2013). Evidence of syndepositional extension, including growth strata and angular unconformities between each formation, indicates that these half-graben basins began to form by the time the upper part of the Parajes formation was erupted (ca. 27.5 Ma) and continued to develop during deposition of the Témoris and Sierra Guazapares formations. Several of these preexisting extensional structures controlled the localization of andesitic and silicic volcanic vents and shallow level intrusions of the Témoris and Sierra Guazapares formations (Murray et al., 2013).

3.2. Guazapares Fault Zone

The Guazapares Fault Zone extends from Témoris northward to the Monte Cristo resource area immediately west of a prominent ridge composed of Sierra Guazapares formation rocks (Figs. 1 and 3); the northern and southern limits of the fault zone are not known but it appears to continue beyond the map area, as do the silicic intrusions associated with the mineralized zones, which is important for future prospecting. The Guazapares Fault Zone is a ~3 to 5 km-wide system of NNW-striking normal faults with numerous splays that dip both east and west, with several changes of fault dip polarity along strike. The strikes of the faults in the Guazapares Fault Zone appear to bend slightly west near their northern part close to the Monte Cristo resource area, where the width of the fault zone increases (Fig. 3). The faults in the Guazapares Fault Zone host the majority of the mineralized structures within the mining district, and several resource areas,

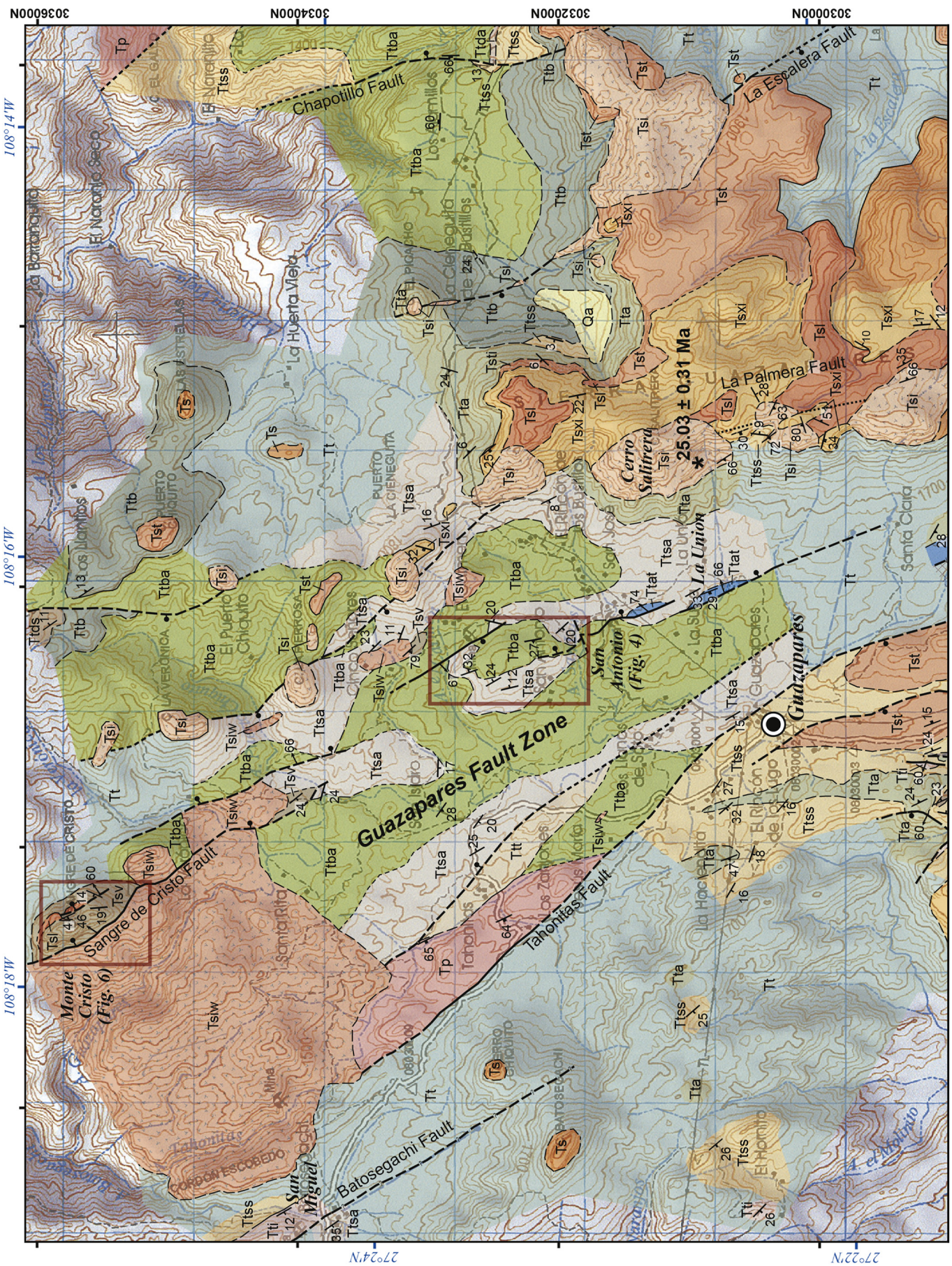

Fig. 3. (*continued*).

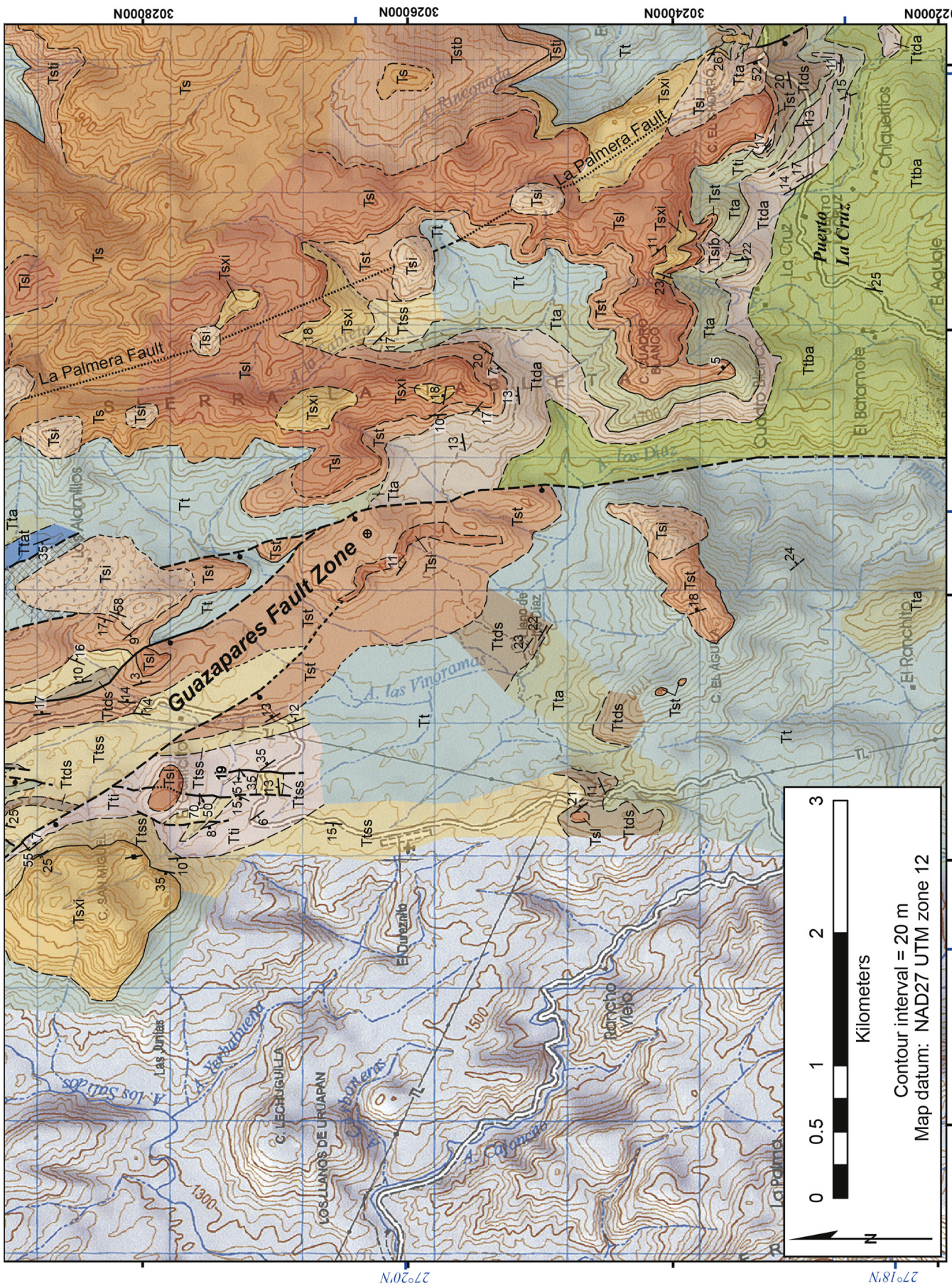

Fig. 3. (*continued*).

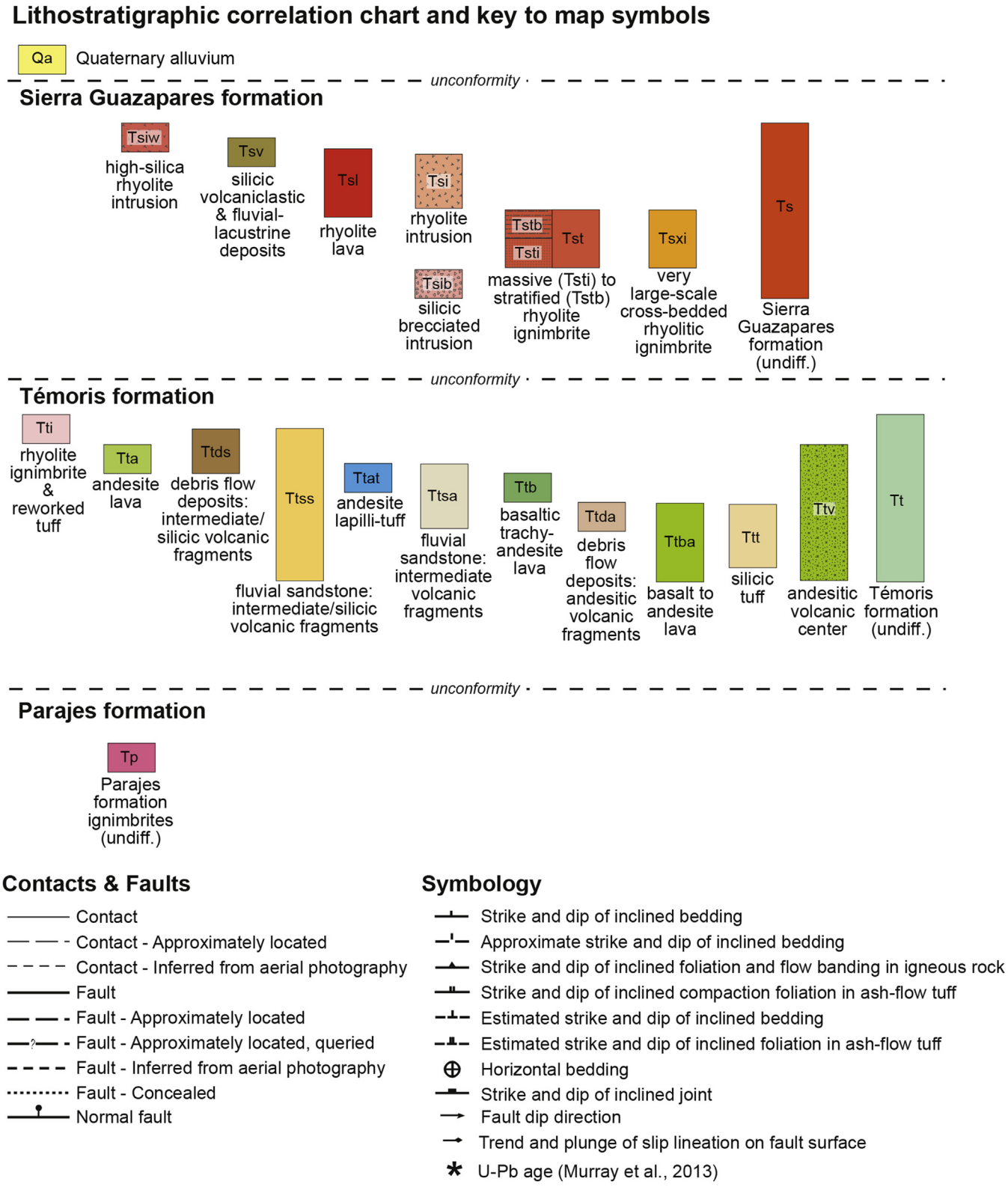

Fig. 3. Geologic map of the Guazapares Fault Zone between Monte Cristo and ~2 km north of Témoris, with lithostratigraphic correlation chart for the map units of the Guazapares Mining District and key to map symbols (after Murray et al., 2013). See Table 1 of Murray et al. (2013) for lithologic descriptions of the map units. Red boxes indicate the locations of Fig. 4 and 6. Resource areas discussed herein are (from north to south): Monte Cristo, San Antonio, and La Unión. Age data are from zircon U–Pb laser ablation ICP-MS geochronology by Murray et al. (2013). (For interpretation of the references to color in this figure legend, the reader is referred to the web version of this article.)

including the San Antonio, Monte Cristo, and La Unión areas (discussed below), are located along a series of faults on the eastern side of the fault zone (Fig. 3) referred to as the "main Guazapares structure" by Roy et al. (2008).

Several mineralized zones are located west of the main Guazapares structure of the Guazapares Fault Zone (Fig. 3). The San Miguel resource area is located along the NW-striking, SW-dipping Batosegachi Fault, which has been interpreted as a right-lateral strike-slip fault with a normal-slip component (D. Sims, pers. commun.). We identified the NW-striking Tahonitas Fault, located between the Batosegachi Fault and main Guazapares structure (Fig. 3). A few currently undeveloped resource areas are located along the Tahonitas Fault (not labeled on Fig. 3); however, it appears to be a major structure within the mining district, with a ~50 m-wide zone of argillic and propylitic alteration and quartz veining that is located on the western edge of a fault-bounded outcrop of Parajes formation ignimbrite (Tp; Fig. 3). The Tahonitas Fault forms a lithologic boundary within the mining district, with the rhyolite ignimbrite-dominated upper section of the Témoris formation located to the southwest of the southern section of the fault and the mafic-to-andesitic-dominated lower and middle sections of the Témoris formation located to the northeast of the structure (Fig. 3).

4. Resource areas of the Guazapares Fault Zone

This study provides new detailed geologic maps and cross-sections of the San Antonio and Monte Cristo resource areas (Figs. 4–8) located along main mineralized structure of the Guazapares Fault Zone (Fig. 3); it also briefly describes the discusses the La Unión resource area, located along the same structure. Our interpretations are based on detailed geologic mapping, used to describe the stratigraphy and structural geology of each resource area.

4.1. San Antonio resource area

The San Antonio resource area (Fig. 4) lies along the Guazapares Fault Zone approximately 2 km NNE of Guazapares (Fig. 3). Previous mining company reports have identified an approximately 350 m-wide by 1 km-long mineralized zone within the center of the San Antonio resource area, with subvertical NW-trending mineralized structures that are steeply west-dipping in the north and steeply east-dipping in the south (Roy et al., 2008; Gustin, 2012). Based on our study, we interpret this resource area to be the location of an accommodation zone between two opposite dipping normal faults that hosts mineralization (Fig. 5).

The rocks exposed at the San Antonio resource area are part of the lower section of the Témoris formation, consisting of mafic to intermediate composition lavas and autoclastic flow breccias (Ttba), interstratified with lithic-rich sandstone with mafic to intermediate volcanic rock fragments (Ttsa) and lesser silicic lapilli-tuff (Ttt) (Table 1). The lavas laterally interfinger with the sandstones and infill channels, and sandstones occur as lenses within the lavas and locally have trough cross-bedding and gravel lenses. The presence of these sedimentary structures and the channelization of deposits suggest deposition in a fluvial environment (Fig. 5A).

The main geologic structures in the San Antonio resource area are two NW-trending normal faults with opposing dip directions: a W-dipping fault in the northern section of the area and an E-dipping fault in the southern section, separated laterally by ~400 m (Fig. 4). The volcanic and sandstone deposits of the Témoris formation are tilted toward each of these normal faults, resulting in opposite bedding dip directions in the northern and southern sections of the resource area (Fig. 4). We interpret the area between these two normal faults, where the dip orientation of the faults and bedding changes, as an antithetic accommodation zone dominated by extensional deformation with negligible strike-slip motion (e.g., Faulds and Varga, 1998).

The majority of mineralization in the San Antonio resource area is concentrated in the antithetic accommodation zone in the center of the area, between the two main normal faults (Figs. 4 and 5). The volcanic rocks are weakly altered to unaltered in the northern and southern sections of the area and are strongly silicified towards the center of the area (Fig. 4), with mineralization dominated by silver (~10% gold) and occurring as subvertical NW-trending vuggy and banded quartz/chalcedony-amethyst veinlet stockworks and rare discrete quartz veins (Gustin, 2012). The location of the antithetic accommodation zone corresponds with this zone of silicification, suggesting that subvertical dilational structures formed in the area between the two normal faults during continued extension (Fig. 5B); these influenced the localization of mineralization by opening up NW-trending cracks that provided conduits for mineralizing fluids. As discussed below, this extension and mineralization probably occurred during emplacement of silicic intrusions of the Sierra Guazapares formation.

4.2. Monte Cristo resource area

The Monte Cristo resource area (Fig. 6) lies along the northern mapped portion of the Guazapares Fault Zone, approximately 5.5 km NNW of Guazapares (Fig. 3). The main geologic structure in the resource area is the Sangre de Cristo Fault, which is a NNW-striking, E-dipping normal fault that juxtaposes a white, highly-altered rhyolite hypabyssal intrusion in the footwall with much less altered dominantly rhyolite volcaniclastic fill on the hanging wall (Figs. 6 and 7A). Zircon U–Pb laser ablation ICP-MS geochronology by Murray et al. (2013) and our new geologic mapping here shows that the rocks in the Monte Cristo resource area record deposition of the Sierra Guazapares formation (ca. 23 Ma) in a synvolcanic half-graben that formed within an actively growing rhyolite dome-hypabyssal intrusive complex (Figs. 7 and 8). The footwall of the Sangre de Cristo Fault consists of a subvolcanic intrusion of white high-silica rhyolite (Murray et al., 2013), which is aphyric and subvertically flow-banded (Tsiw; Fig. 7B; Table 1). This hypabyssal rock intrudes gray andesitic feldspar porphyry of the Témoris formation and is offset by the Sangre de Cristo Fault, indicating emplacement prior to the most recent motion along this fault. The white high-silica rhyolite intrusion in the footwall of the Sangre de Cristo Fault hosts most of the multi-phase gold–silver-bearing mineralization in the Monte Cristo resource area (Gustin, 2012), with subvertical quartz veins striking both northwest and northeast. The northeast vein orientation appears to be unique to the Monte Cristo resource area, since mostly NW-striking veins are found in the other resource areas within the Guazapares Mining District. Three major quartz veins that cut the white rhyolite intrusion in the footwall block are sited along small-offset NE-striking faults that terminate at the Sangre de Cristo Fault (Fig. 6), suggesting that the age of quartz mineralization of these veins predates the most recent motion on the Sangre de Cristo Fault. Siliceous sinter mineralization in the hanging wall is limited to rocks within ~10 m of the Sangre de Cristo Fault, which may have served as a conduit for to silica-rich mineralizing fluids migrating up the basin margin (Gustin, 2012). The footwall hypabyssal intrusion presently crops out over an area of ~8 km^2 (see Tsiw, Fig. 3), which is too large to feed to a single lava dome. We infer that the white high-silica rhyolite hypabyssal intrusion represents a high-level subvolcanic magma chamber that had several feeder plugs above it that fed an overlying lava dome field; this dome field

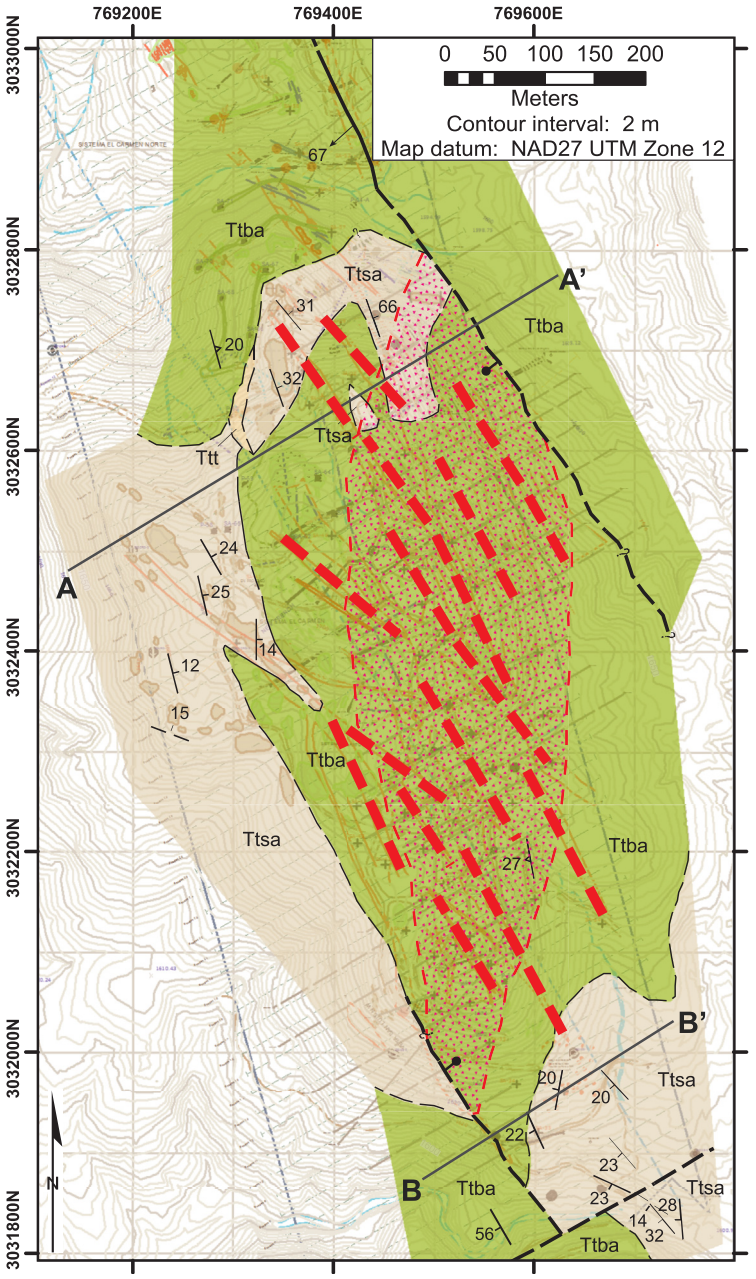

San Antonio resource area

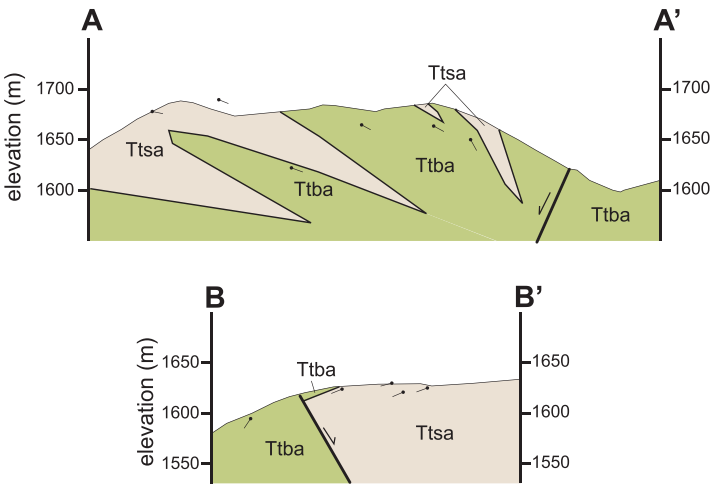

Lithostratigraphic correlation chart and key to map symbols:

Témoris formation

Ttba	Ttsa	Ttt
basalt to andesite lava	fluvial sandstone: intermediate volcanic fragments	silicic tuff

Contacts & Faults

- Contact - Certain
- Contact - Approximately located
- Contact - Approximately located, queried
- Fault - Certain
- Fault - Approximately located
- Fault - Approximately located, queried
- Normal fault - tick mark on hanging wall

Symbology

- Fault dip direction
- Strike and dip of inclined bedding
- Approximate strike and dip of inclined bedding
- Strike and dip of flow-banding in igneous rocks
- Intensely veined accommodation zone in region of normal fault tilt inversion, dashed lines indicate major veins (Roy et al., 2008).
- Projected dip amount on cross-sections

Fig. 4. Geologic map and cross-sections of the San Antonio resource area of the Guazapares Fault Zone (Fig. 3). The red striped area indicates the region of intense epithermal mineralization with subvertical NW-trending vuggy and banded quartz/chalcedony-amethyst veinlet stockworks and rare discrete quartz veins in the accommodation zone between two normal faults with opposing dip directions. Cross-sections A–A′ and B–B′ of the San Antonio resource area based on surficial geologic mapping, showing the change in normal fault and bedding dip orientations between the northern and southern portions of the resource area. Base map from (Roy et al., 2008). Descriptions of the lithologic units are given in Table 1. (For interpretation of the references to color in this figure legend, the reader is referred to the web version of this article.)

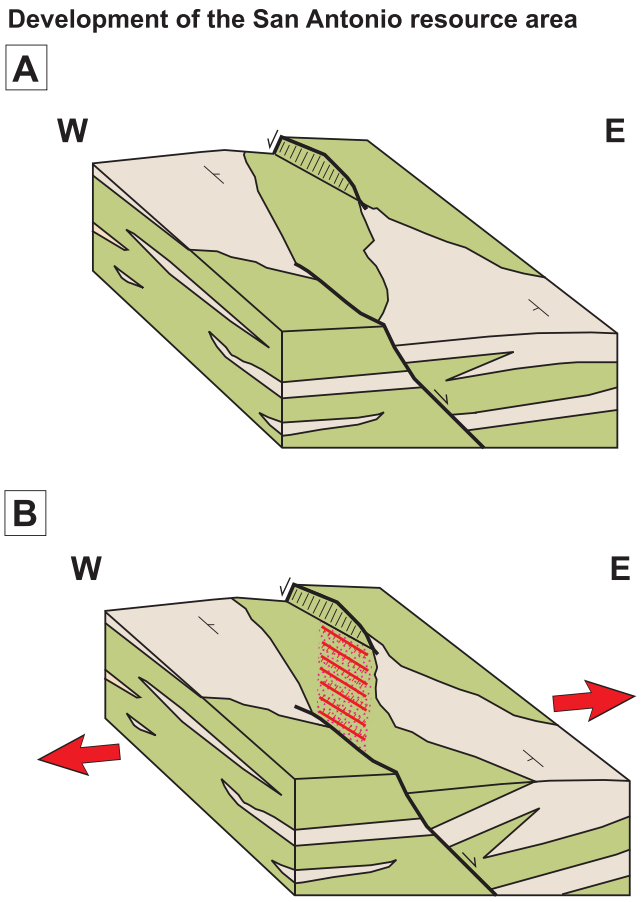

Fig. 5. Schematic block diagrams illustrating the evolution of the San Antonio resource area. Colors correspond to the geologic map units in Fig. 4. (A) Lava, sandstone, and lesser silicic tuff of the Témoris formation were deposited in a fluvial environment and offset across the two normal faults (a W-dipping fault in the north and E-dipping fault in the south). (B) Continued NE–SW-directed extension resulted in the formation of subvertical NW-trending dilational structures (red lines, hash marks indicated dip direction) in the antithetic accommodation zone between the two normal faults. This accommodation zone corresponds with a zone of intense silicic alteration (red triangles) within the resource area. (For interpretation of the references to color in this figure legend, the reader is referred to the web version of this article.)

in turn shed dome collapse breccias and block-and-ash flows into the adjacent half-graben basin (Fig. 8). Continued extensional deformation on the Sangre de Cristo Fault led to uplift and erosion of the domes and feeder plugs, resulting in unroofing of the high-level subvolcanic magma chamber, and shedding of the erosional material into the basin (Fig. 8).

4.2.1. Sangre de Cristo Fault half-graben basin development

The dominant unit in the hanging wall of the Sangre de Cristo Fault is a massive rhyolitic breccia (Tsvdb, Tsvdl; Table 1) located adjacent to the fault (Fig. 6). Although mining company reports have described this as a hydrothermal breccia, we interpret the massive rhyolitic breccia as a lava dome-collapse volcanic breccia, derived directly from a concurrently growing rhyolite dome-hypabyssal intrusion complex that was located on the footwall of the Sangre de Cristo Fault (Fig. 8B); the lava dome-collapse breccia lacks quartz veining and secondary silicification in the groundmass (except within 10 m of the Sangre de Cristo Fault) that is typical of hydrothermal breccias. The massive rhyolitic breccia is very similar in appearance to the white high-silica rhyolite intrusions in the footwall of the Sangre de Cristo Fault; it is white, angular, predominantly block-supported, and monomictic, composed of aphyric to weakly porphyritic rhyolite, with minor flow-banded blocks, and an ash matrix of the same composition (Fig. 7C). Locally, the breccia contains up to 20% andesitic blocks, likely entrained into lava dome-derived avalanches as they traversed the normal fault scarp to enter the graben. The rhyolite block fragment size decreases rapidly away from the Sangre de Cristo Fault, from >2 m blocks adjacent to the fault to lapilli-sized fragments ~200 m from the fault towards the northeast. We interpret this unit as dome collapse breccias that avalanched off of a growing rhyolite dome-hypabyssal intrusion complex, which was located on the footwall of the Sangre de Cristo Fault, shedding rhyolite blocks into the adjacent half-graben basin (Fig. 8B). We consider this deposit to represent a dome collapse breccia rather than a fault talus breccia because it is monomictic, with limited accidental andesitic clasts, and the lapilli-to-ash-sized fragments are identical in composition to the blocks (rhyolitic). The clast-supported nature of most of the dome collapse breccia is that of a hot-block-avalanche deposit in a position proximal to one or more growing lava domes, and the lapilli-to ash-sized fragments of this breccia are typical of proximal block-and-ash-flow tuffs, also produced by lava dome collapse (e.g., Fisher and Schmincke, 1984; Freundt et al., 2000). The age of a rhyolite block within this dome collapse breccia has been dated at 24.2 ± 0.2 Ma by U–Pb zircon LA-ICP-MS (Murray et al., 2013), showing it is part of the Sierra Guazapares Formation, which is dominated by vent facies silicic volcanic rocks.

The rhyolitic dome collapse breccias overlie, and the basal deposits interfinger with, sedimentary rocks that we infer to be lacustrine deposits (Fig. 8A–B). The lacustrine sedimentary rocks outcrop on the eastern side of the Monte Cristo resource area (Fig. 6), and consist of mudstone, normal-graded sandstones, and well-laminated subaqueous fallout tuff (Tsvl; Table 1; Fig. 7D). The light gray turbiditic fine-to-medium-grained sandstones exhibit Bouma sequences A and B (Fig. 7D), and grade upward into planar finely laminated to very thinly bedded mudstone and tuffs. The presence of lacustrine sedimentary rocks at the base of the section below the lowest rhyolite breccia (but also interfingering with it) suggests that extension and half-graben formation preceded the onset of silicic magmatism at this locality. Soft-sediment deformation structures are present (Fig. 7E), suggesting that these lacustrine deposits were deformed by seismicity related to fault motions and/or volcanic activity.

The dome collapse breccias pass gradationally upward and outward (Figs. 6 and 8C) into a predominantly massive monomict silicic lithic lapilli-tuff unit (Tsvm; Table 1). This lithologic unit is primarily gray to very light red lapilli-tuff with angular rhyolite clasts similar to those in the breccia. We interpret the massive lapilli-tuff unit to represent distal equivalents of the block-and-ash-flow deposits present in the breccia unit, perhaps shed from a lava dome that was slightly more distal from the basin. Locally interbedded with the massive silicic lapilli-tuff unit are light gray, massive, moderately to poorly sorted, medium-to-coarse-grained sandstones and conglomerates (Tsvf; Table 1), which are also dominated by crystal-poor rhyolite, but have a higher degree of sorting and more rounding of grains. These sandstones and conglomerates also have cut-and-fill structures and trough cross-bedding indicating fluvial deposition. The sandstones could represent material reworked from unconsolidated primary volcanic deposits, or they could record erosion of the lava domes, but their monomict character indicates a very restricted source area (i.e., the rhyolite dome field).

Interstratified with the massive silicic lapilli-tuff unit (Tsvm) in the northern part of the Monte Cristo resource area is a white to gray silicic lava flow (Tsl; Table 1) that continuously transitions into a feeder dike (Figs. 6 and 8E). This silicic lava differs in appearance from the aphyric rhyolitic hypabyssal intrusions in footwall block

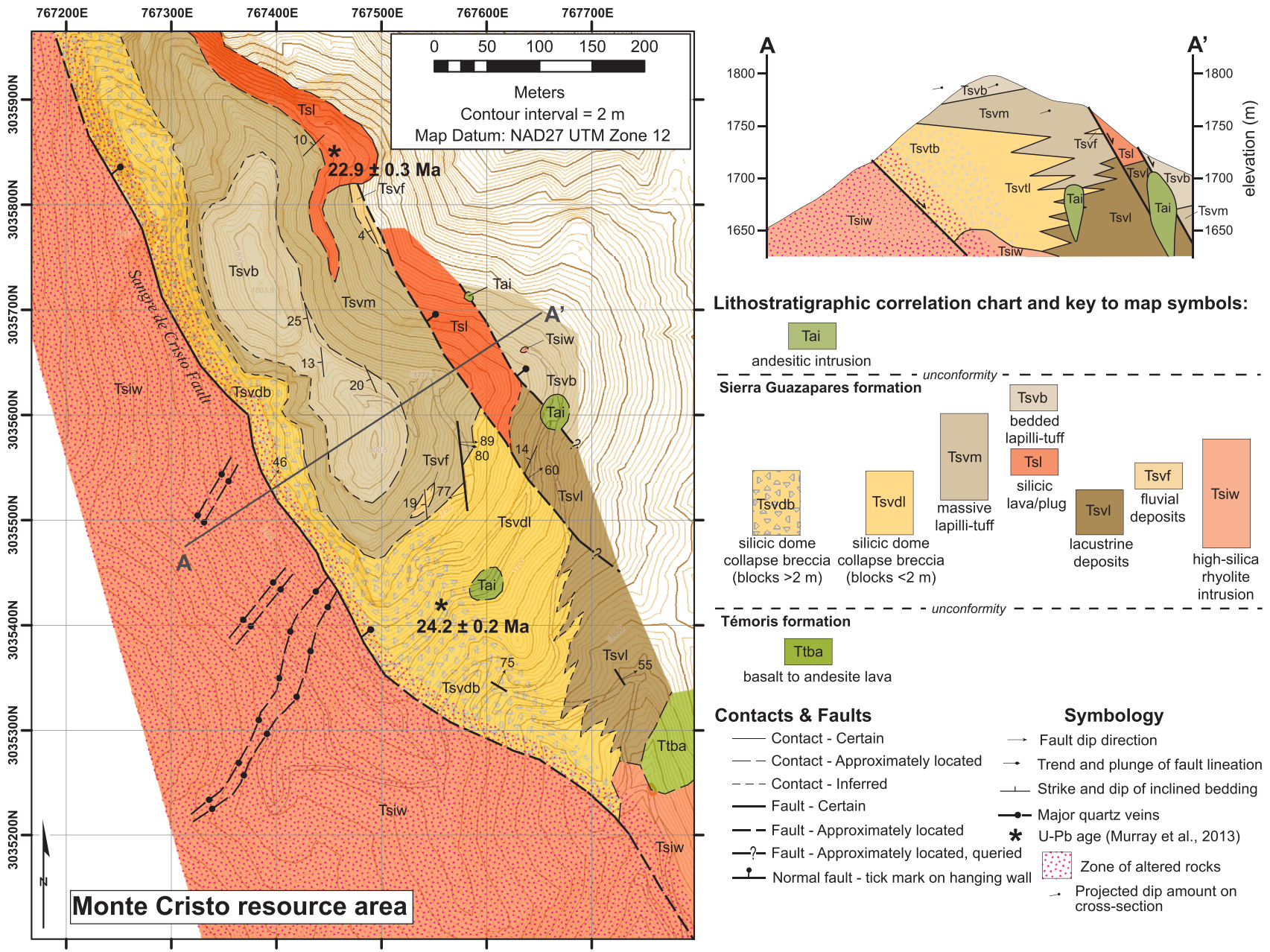

Fig. 6. Geologic map and cross-section of the Monte Cristo resource area, with volcanic and volcaniclastic sedimentary rocks located on the hanging wall of the east-dipping Sangre de Cristo Fault and a rhyolite intrusion in the footwall. Cross-section A–A′ of the Monte Cristo resource area based on surficial geologic mapping, showing the distribution and depositional relationships of the synvolcanic half-graben deposits. Reddish-pink triangles denote the region of heavy quartz mineralization of the footwall and within ~10 m of the Sangre de Cristo Fault. Descriptions of the lithologic units are given in Table 1. (For interpretation of the references to color in this figure legend, the reader is referred to the web version of this article.)

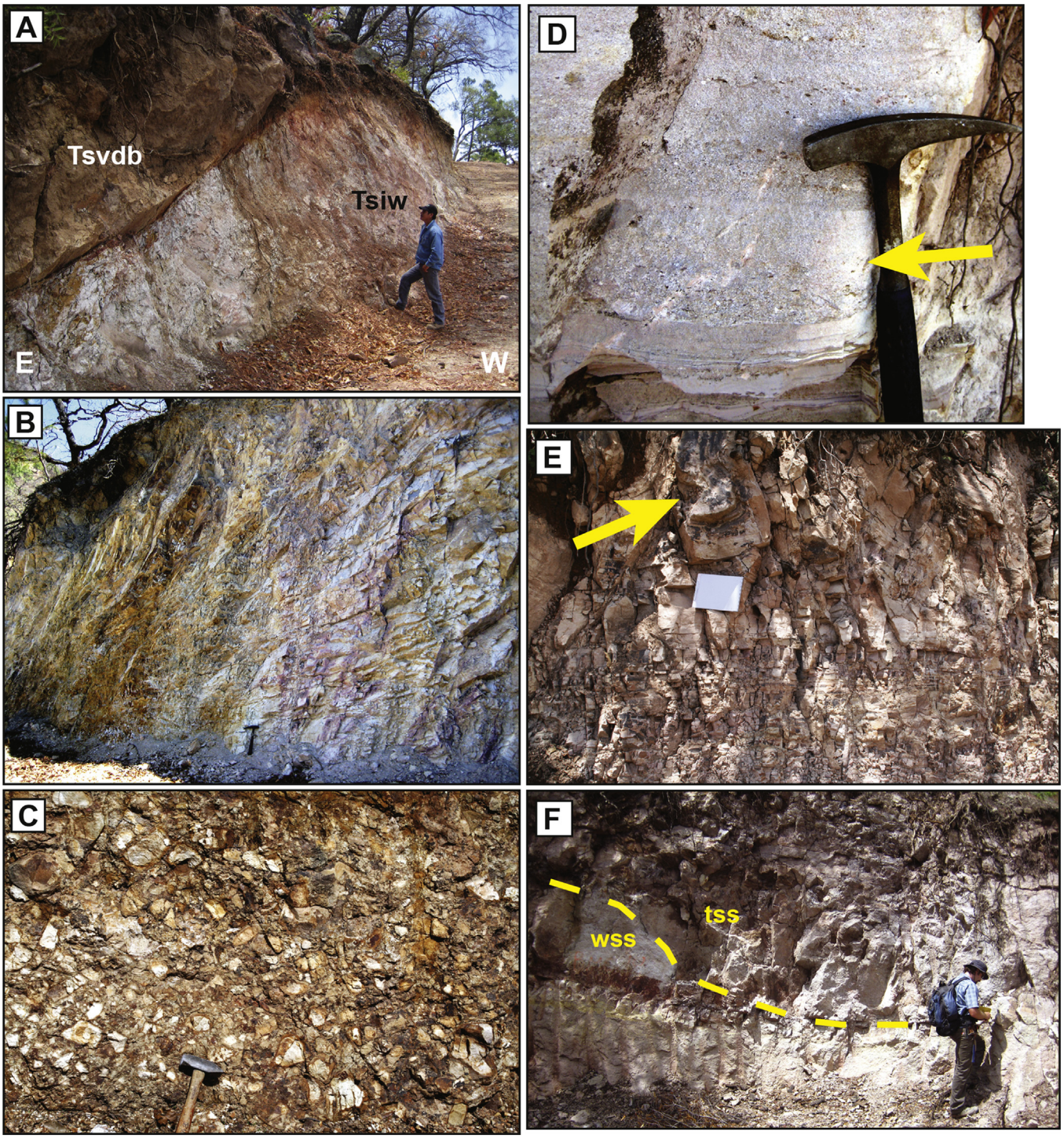

Fig. 7. Photographs from the Monte Cristo resource area; locations of photos given (NAD27 UTM zone 12). All map units referred to here are shown on Fig. 6. (A) The Sangre de Cristo Fault in the northwestern section of the resource area, with white aphyric high-silica rhyolite intrusion (Tsiw) in the footwall (right) and tan hematized rhyolitic dome collapse breccia (Tsvdb) in the hanging wall (left). Photograph taken at 767366E 3035552N. (B) White aphyric high-silica rhyolite intrusion (Tsiw) from the roots of the rhyolite dome-hypabyssal intrusion complex in the footwall of the Sangre de Cristo Fault. Subvertical flow-banding visible on left side of photograph. Hammer (33 cm-tall) for scale. Photograph taken at 767764E 3035213N. (C) White rhyolitic dome collapse breccia (Tsvdl) on the hanging wall of the Sangre de Cristo Fault, showing primarily monomictic composition similar in appearance to the footwall rhyolite intrusions, with a small percentage of dark-colored andesitic blocks. Groundmass is composed of the same material as the rhyolitic blocks. Head of hammer is ~12.5 cm. Photograph taken at 767632E 3035526N. (D) Turbiditic fine-to-medium-grained sandstone exhibiting graded bedding with Bouma sequence A and B (arrow) in lacustrine sedimentary unit (Tsvl) in the basal half-graben fill on the hanging wall of the Sangre de Cristo Fault. Laminated mudstone and water-laid tuff layers underlie the turbiditic sandstone. Hammer head (~17.5 cm-length) for scale. Photo taken at 767640E 3035559N. (E) Soft sediment folding (arrow, above ~30 cm-length notebook) in mudstone in the basal lacustrine half-graben fill (Tsvl), on the hanging wall of the Sangre de Cristo Fault. Photo taken at 767641E 3035551N. (F) Bedded lapilli-tuff unit (Tsvb) in the half-graben fill on the hanging wall of the Sangre de Cristo Fault. A cut-and-fill structure (yellow dashed line) truncates the underlying white tuffaceous sandstone (wss) and is filled with coarse sandstone (tss). Photograph taken at 767486E 3035634N. (For interpretation of the references to color in this figure legend, the reader is referred to the web version of this article.)

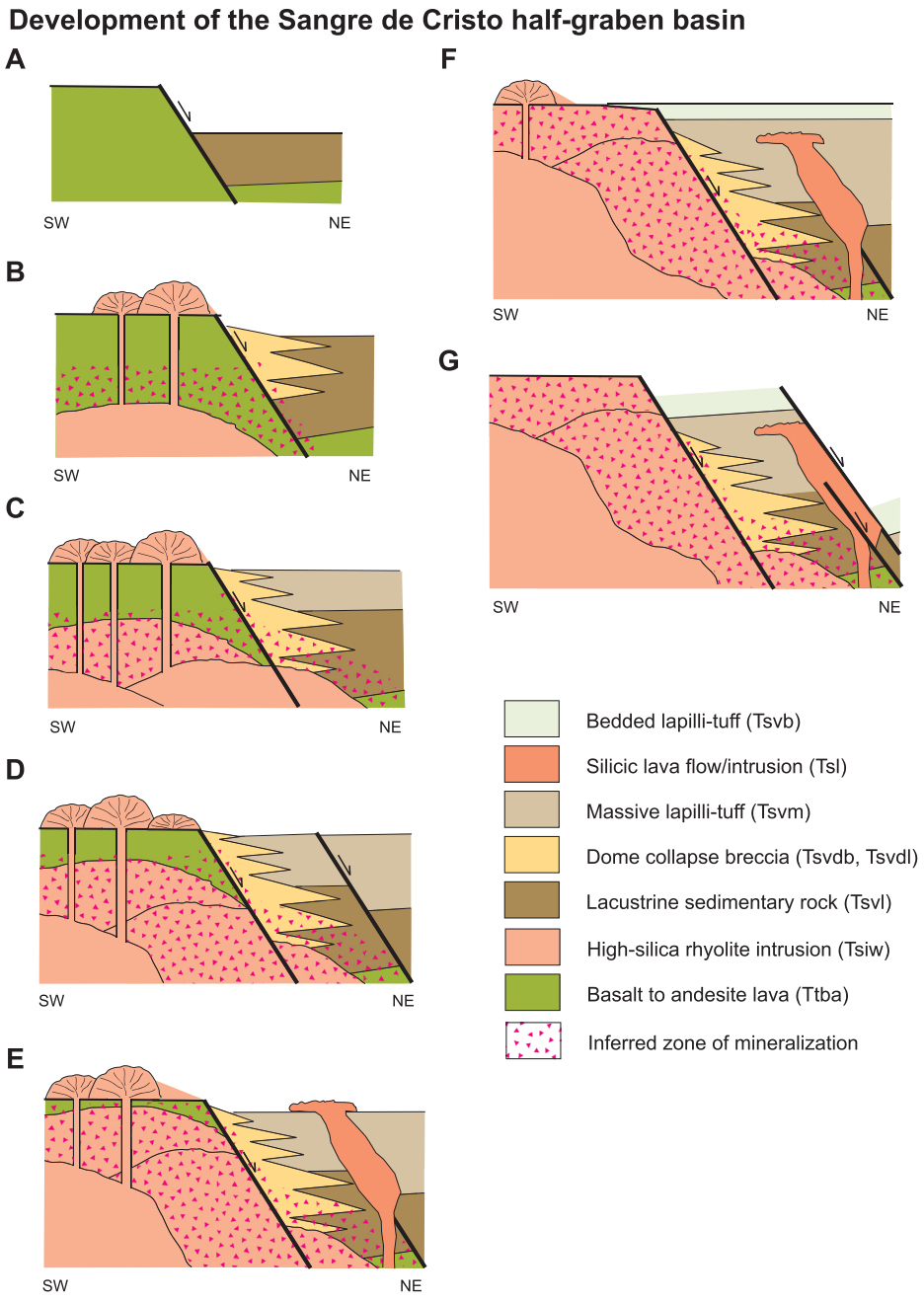

Fig. 8. Interpretive cross-section diagrams (not to scale) showing the phases of basin development and inferred timing of magmatism and mineralization within the Monte Cristo resource area. Active faulting is denoted with arrows. (A) Initial motion along the Sangre de Cristo Fault created a small half-graben basin, in which lacustrine sediments (Tsvl) were deposited. (B) Collapse of a rhyolite dome located on the footwall of the Sangre de Cristo Fault shed blocks into the subsiding basin (Tsvdb, Tsvdl), interfingering with, and prograding over the lacustrine deposits. Emplacement of the white rhyolite intrusion (Tsiw) located on the footwall of the Sangre de Cristo Fault is likely related to the eruption of a rhyolite dome complex that shed material into the half-graben basin; the emplacement of these hypabyssal intrusions likely mineralized the Témoris formation in the footwall and the adjacent half-graben basin fill. (C) Growth of the rhyolite dome-hypabyssal intrusion complex on the footwall led to continued deposition of dome collapse breccias in the Sangre de Cristo half-graben (Tsvdb, Tsvdl), which transition northeastward into block-and-ash flow deposits and lesser reworked tuff of the massive silicic lapilli-tuff unit (Tsvm). Younger rhyolite intrusions mineralized the older intrusions in the footwall and the half-graben fill adjacent to the bounding fault. (D) Syndepositional normal faulting within the hanging wall block developed concurrently with deposition of the massive lapilli-tuff unit. (E) Emplacement of a silicic plug and coulee (Tsl) along the normal fault within the hanging wall block during deposition of the massive lapilli-tuff unit. (F) Deposition of the bedded lapilli-tuff unit (Tsvb) records fluvial deposition of detritus shed from the lava dome complex during waning volcanism, or during migration of lava dome volcanism away from the basin. (G) Postdepositional normal faulting on the Sangre de Cristo Fault, and smaller faults within the hanging wall, tilted the strata, offset the white rhyolite intrusion and silicic plug/coulee, and down-dropped the bedded lapilli-tuff unit to the east.

and the blocks of the dome collapse breccia and lapilli tuffs; in comparison, this unit is crystal-poor, with ~5% plagioclase and biotite and trace hornblende. The extrusive lava part of this unit is thick and stubby, which is interpreted as a coulee (e.g., Fink and Anderson, 2000). The top surface of the coulee is slightly irregular with planar thinly bedded very fine-to-fine-grained sandstone and tuff layers filling in the depressions between it and the overlying massive lapilli-tuff unit. The age of this lava flow is 22.9 ± 0.3 Ma by U–Pb zircon LA-ICP-MS (Murray et al., 2013). The feeder dike of this coulee follows a normal fault that offsets the massive silicic lapilli-tuff unit (Figs. 6 and 8D, E); this supports our interpretation that extension and rhyolite intrusive activity were

coeval since this dike follows a pre-existing normal fault (Fig. 8E) and is in turn cut by another fault (Fig. 8G).

The massive silicic lapilli-tuff unit (Tsvm) passes gradationally upward into a bedded silicic lapilli-tuff unit (Fig. 8F), composed of well-stratified silicic lapilli-tuff, tuff and sandstone (Tsvb: Table 1). The clasts are dominantly composed of the same crystal-poor rhyolite present in the massive silicic lapilli-tuff (Tsvm) and the dome-collapse breccia (Tsvdb, Tsvdl) units, but is finer grained, better sorted, subangular to subrounded, and has abundant sedimentary structures typical of fluvial deposition, such as cut-and-fill structures and planar-lamination (Fig. 7F). We interpret this unit to record fluvial deposition of detritus eroded from the lava dome complex during waning volcanism, or during migration of lava dome volcanism away from this part of the basin (Fig. 8F). The bedded lapilli tuff is offset by a second intrabasinal normal fault (Fig. 8G).

Some footwall uplift must have occurred after emplacement of the bedded lapilli tuff unit, as the youngest exposed units are tilted; however, we infer that most of the displacement on the Sangre de Cristo Fault occurred during formation of the half-graben, emplacement of the dome-hypabyssal intrusion complex, and mineralization (Fig. 8).

4.3. La Unión resource area

Like the San Antonio and Sangre de Cristo resource areas, the La Unión resource area is located on the eastern edge of the Guazapares Fault Zone, close (<1 km) to the Sierra Guazapares formation plugs exposed along the La Palmera Fault to the east (Fig. 3). We did not map this area in detail, as there were no detailed topographic maps constructed for it like there were at the other two resource areas, nor does it contain numerous rock exposures along road cuts that are typical in the other resource areas.

The rocks exposed at the La Unión resource area are similar to those of the San Antonio resource area to the north, consisting of Témoris formation mafic to intermediate composition lava and flow breccia (Ttba), andesitic volcanic lithic-rich sandstone (Ttsa), andesitic lapilli-tuff (Ttat), and lesser silicic tuffs (Fig. 3). Mineralization in the La Union resource area consists of locally intense multi-phase brecciation and silicification grading laterally into quartz-veinlet stockwork zones (Gustin, 2012). The main structures that host the mineralization are two NNW-trending, E-dipping normal faults, offset laterally by ~100 m (Fig. 3); smaller mineralized structures are located at this offset, which is likely a synthetic accommodation zone (e.g., Faulds and Varga, 1998) between these two faults.

Located less than 1 km to the east of the La Unión resource area is Cerro Salitrera, one of the largest silicic intrusions (~0.6 km^2) of the Sierra Guazapares formation intruded along the La Palmera Fault (Fig. 3). We suggest that mineralization in the La Unión resource area is likely related to the close proximity of the Cerro Salitrera plug. As reported in an unpublished mining company report (Gustin, 2012), the inferred gold concentration in the La Unión resource area is one of the highest in the Guazapares Mining District (~35 g Au/ton), with much lower gold concentrations away from this intrusion (i.e., ~10 g Au/ton at the San Antonio resource

Table 1
Lithologic units of the San Antonio & Monte Cristo resource areas.

Map unit[a]	Lithology	Description
Tai	Andesitic intrusions	Hypabyssal intrusion. Dark gray with local red hematitic & green propylitic alteration; aphanitic groundmass with 5–10% phenocrysts: plagioclase, clinopyroxene.
Tsvb	Bedded silicic lapilli-tuff	Silicic lapilli-tuff. Light red to gray; nonwelded; <5% phenocrysts: plagioclase, biotite; up to 20% lithic fragments (intermediate volcanic). Fluvial reworking with bedding structures (planar lamination, cut-and-fill structures), bedding up to 2 m thick. Local white reworked tuff layers.
Tsl	Rhyolite lava/intrusion	Lava flow & hypabyssal intrusion. White to light gray, with light pink flow banding; 5% phenocrysts: plagioclase, biotite, trace hornblende. Irregular top surface of flow.
Tsvf	Fluvial sandstone: silicic volcanic fragments	Feldspathic litharenite. White to light gray; moderately to poorly sorted, subangular, medium-to-coarse-grained. Clast consist of silicic lithic fragments and feldspar. Massive with faint laminations, also contains cut-and-fill and trough cross-bedding structures. Minor clast-supported breccia with subangular cobble-boulder silicic lapilli-tuff fragments. Interpreted as hyperconcentrated debris flows of reworked silicic volcanic material.
Tsvm	Massive silicic lapilli-tuff	Silicic lapilli-tuff. Light red to gray; nonwelded; <5% phenocrysts: plagioclase, biotite; trace lithic fragments (intermediate volcanic). Slight fluvial reworking with crude bedding up to 5 m thick. Local red very fine-grained, thinly bedded sandstone.
Tsvdb; Tsvdl	Rhyolitic dome collapse breccia	Dome collapse block-and-ash flow breccia. White to light orange; primarily monolithic rhyolite breccia, block-supported, angular blocks (>2 m), lesser flow-banded blocks. Blocks are aphyric, with trace quartz and plagioclase phenocrysts, in an ash-lapilli groundmass of same composition. Contains local zones of up to 20% intermediate blocks. Block breccia (Tsvdb) transitions laterally into lapilli breccia (Tsvdl) of same composition. The block fragment size decreases northeastward away from the Sangre de Cristo Fault, from >2 m blocks to lapilli-sized fragments supported in an ash matrix. Fragments are similar in appearance to high-silica rhyolite intrusion (Tsiw).
Tsiw	High-silica rhyolite intrusion	Hypabyssal intrusion (dome/plug). White to light pink; aphyric to 10% phenocrysts (up to 1 mm): plagioclase, biotite, trace quartz. Subvertical flow banding. Intruded into gray andesitic feldspar porphyry (likely part of Témoris formation). Similar in appearance to rhyolitic dome collapse breccia (Tsvd).
Tsvl	Lacustrine sandstone & mudstone	Mudstone and sandstone. Tan to white. Sandstone: Feldspathic litharenite; fine-to-medium-grained sandstone with graded bedding (Bouma Sequence A, B) and small scale basal scouring. Mudstone: planar laminated to very thinly bedded, contains thin tuff layers. Soft sediment slumping and folding.
Ttba	Basalt to andesite lava	Predominantly amygdaloidal lava flows. Gray to dark gray with local red hematitic & green propylitic alteration; 5–25% phenocrysts: plagioclase (some flow-alignment of laths), clinopyroxene; zeolite amygdules. Average lava flow thickness ~5 m, lavas are typically brecciated and vesicular with secondary zeolite infilling vesicles and autoclastic flow breccia interstices fragments, with lesser flow-banded and nonvesicular lavas with flow-top and bottom autoclastic breccias.
Ttsa	Fluvial sandstone: intermediate volcanic fragments	Feldspathic litharenite. Dark tan to reddish purple; moderately to poorly sorted, subrounded to subangular, medium-to-coarse-grained with trace granules. Clasts consist of feldspar and intermediate volcanic lithic fragments. Contains lenses of clast-supported pebble conglomerates and matrix-supported pebble to cobble breccia with intermediate volcanic fragments. Thinly to thickly bedded.
Ttt	Silicic tuff	Nonwelded to partially welded tuff. White to light tan groundmass; trace-10% phenocrysts (<1 mm): plagioclase, biotite, ±hornblende, ±quartz; trace to 25% lapilli-sized lithic fragments (red intermediate volcanic).

[a] Figs. 4 and 6.

area); however, this report does not recognize the Cerro Salitrera plug, nor does it relate the mineralization to proximity to the intrusion.

5. Discussion

This study shows that mineralization in the Guazapares Mining District was directly related to Late Oligocene to Miocene silicic magmatism of the mid-Cenozoic ignimbrite flare-up of the Sierra Madre Occidental at ca. 24.5–23 Ma (Sierra Guazapares formation). The epithermal deposits in the study area are related to the emplacement of Sierra Guazapares formation rhyolite hypabyssal intrusions less than 2 Myr after deposition of the Témoris formation, with normal faults and accommodation zones providing conduits for intrusion-related hydrothermal fluids and a location for precious metal mineralization. The geology of three resource areas along the Guazapares Fault Zone presented in this study supports the interpretation that rhyolite hypabyssal intrusions are related to mineralization along preexisting extensional structures. In the Monte Cristo resource area, deposition in the hanging wall of a synvolcanic half-graben was concurrent with the development of a rhyolite lava dome-hypabyssal intrusion complex in the footwall. Postvolcanic extensional deformation unroofed the top of a subvolcanic rhyolite magma chamber that is now exposed at the surface in the footwall of the Sangre de Cristo Fault. Mineralization emanates upward from the high-silica rhyolite intrusions and is concentrated in the footwall and along the Sangre de Cristo Fault and adjacent hanging wall graben fill. There are no silicic intrusions at the surface within the San Antonio and La Unión resource areas; however, they crop out ~0.5–1 km to the east, where they intruded along the La Palmera Fault. In comparison to the Monte Cristo resource area, these hypabyssal intrusions are exposed at the shallower feeder plug level, suggesting that at least some of the plugs probably unite downward into a larger magma body and that the San Antonio and La Unión resource areas are likely closer to silicic intrusions than surface mapping indicates. Drill core data from Paramount Gold & Silver supports this interpretation, indicating that subsurface silicic intrusions are located at ~120 m-depth beneath the San Antonio resource area and at ~40–90 m-depth beneath the La Unión resource area (Roy et al., 2008).

Similar associations between silicic magmatism, mineralization, and extensional structures have been recognized in other mining districts within the Sierra Madre Occidental, notably in the districts of the Cuenca de Oro basin located ~60 km southeast of the Guazapares Mining District, and the San Martín de Bolaños and Guanajuato districts in the southern region of the Sierra Madre Occidental (Fig. 1). The Cuenca de Oro basin is includes the El Sauzal, Batopilas, and Piedras Verdes mining districts (Sellepack, 1997; Feinstein, 2007). Epithermal mineralization within these mining districts is generally hosted along north-to-northeast-trending fractures and faults in intermediate igneous rocks that appear related to extension in the region (Wilkerson et al., 1988; Goodell, 1995; Sellepack, 1997; Galván-Gutiérrez, 2005; Feinstein, 2007). The highest degree of epithermal mineralization in the Batopilas Mining District is concentrated around the Laramide-age Tahonas granodiorite, which is interpreted as the hydrothermal heat source in the district during and slightly following emplacement of the intrusion (Wilkerson et al., 1988). Further south in the Sierra Madre Occidental in the San Martín de Bolaños Mining District, epithermal mineralization that is hosted primarily in Early Miocene andesitic volcanic rocks occurred between 23.7 and 21.3 Ma; the source of mineralizing fluids is interpreted to be related to a rhyolitic intrusion emplaced in the western escarpment of the Bolaños graben (Scheubel et al., 1988). The timing of mineralization and emplacement of the rhyolitic intrusion in the San Martín de Bolaños Mining District generally corresponds to the Early Miocene pulse of ignimbrite flare-up volcanism that occurred throughout the Sierra Madre Occidental (e.g., Ferrari et al., 2007). However, unlike in the Guazapares Mining District, the mineralized structures observed in this district appear to be unrelated to major extension of the Bolaños graben, which occurred later between 22 and 18 Ma (Scheubel et al., 1988; Ferrari et al., 2007). The Guanajuato Mining District in the southeastern region of the Sierra Madre Occidental has a mineralization history more similar to the Guazapares Mining District. Epithermal mineralization in this district is hosted in NW to NE-trending regional extensional fault systems; the timing of this mineralization is closely associated with magmatic and hydrothermal activity related to the mid-Oligocene emplacement of rhyolite domes near the intersection of these pre-existing regional fault systems (Randall et al., 1994).

Our study shows a direct relationship between silicic intrusion emplacement, epithermal mineralization, and crustal extension in the Guazapares Mining District of the Sierra Madre Occidental. We further show that this occurred during the Early Miocene pulse of the mid-Cenozoic ignimbrite flare-up. Although further research is needed, based on this study and previous studies within the Sierra Madre Occidental, there appears to be at least limited validity to the inferred relationship between epithermal mineralization and major magmatic events in the Sierra Madre Occidental (e.g., Camprubí et al., 2003). Although pre-existing extensional structures are not necessary for the formation of epithermal veins, their presence in this region appears to favor the emplacement of silicic intrusions and provides additional conduits for the circulation and precipitation of mineralized hydrothermal fluids related to these intrusions.

6. Conclusions

1. Three informal Late Oligocene–Early Miocene formations are identified by detailed volcanic lithofacies mapping in the study area: (1) ca. 27.5 Ma Parajes formation, (2) ca. 27–24.5 Ma Témoris formation, (3) ca. 24.5–23 Ma Sierra Guazapares formation. These formations record synextensional deposition and magmatism of the Upper Volcanic Supergroup during the mid-Cenozoic ignimbrite flare-up, and are younger than the previously inferred Eocene age of rocks in the Guazapares Mining District.
2. The majority of epithermal mineralization in the Guazapares Mining District is hosted by the Guazapares Fault Zone, a ~3 to 5 km-wide system of NNW-striking normal faults with east and west dipping splays. The “main Guazapares structure” on the eastern side of the fault zone is the most mineralized area and hosts many of the main resource areas of the mining district (including the San Antonio, Monte Cristo, and La Unión resource areas).
3. Epithermal mineralization in the San Antonio and La Unión resource areas is hosted by Témoris formation lavas and sandstones cut by the main structure of the Guazapares Fault Zone. In the San Antonio resource area, the majority of mineralization is located in an antithetic accommodation zone between two en echelon NW-trending normal faults with opposing dip-directions. The main structures that host mineralization in the La Unión resource area are two NNW-trending, E-dipping normal faults that are offset laterally by ~100 m, with smaller mineralized structures are located in a synthetic accommodation zone between these two faults.
4. The Monte Cristo resource area consists of Sierra Guazapares formation volcanic and volcaniclastic rocks deposited in a synvolcanic half-graben bounded by the Sangre de Cristo Fault during the growth of a rhyolite lava dome-hypabyssal intrusion

complex. Mineralization is concentrated in the high-silica rhyolite intrusions in the footwall and along the syndepositional fault and adjacent hanging wall graben fill.

5. In the Guazapares Mining District, a direct relationship is inferred between the timing of silicic intrusion emplacement, the development of extensional structures, and the localization of epithermal mineralization. Silicic hypabyssal intrusions of the Sierra Guazapares formation are located in close proximity or in the near subsurface of the resource areas studied, with normal faults and accommodation zones providing conduits for intrusion-related hydrothermal fluids and a location for mineralization.

Acknowledgments

For financial, logistical, and intellectual contributions, we thank Paramount Gold & Silver Corp., Larry Segerstrom, Danny Sims, Dana Durgin, Armando Valtierra, and Javier Martínez; we also thank Denis Norton for arranging this support for Busby. Additional financial support was provided by a UC Mexus grant (2009–2010) to Busby and Elena Centeno-García, NSF-EAR-1019559 to Busby, and a GSA student research grant to Murray. Dana Roeber Murray, Jordan Lewis, Adrienne Kentner, and María de los Angeles Verde-Ramírez assisted in the field. We thank the detailed reviews of the manuscript by two anonymous reviewers, and we thank Luca Ferrari, Graham Andrews, Denis Norton, Elena Centeno-Garcia, Martín Valencia, Fred McDowell, Phillip Gans, and John Cottle for informal reviews and discussions.

References

Aguirre-Díaz, G.J., Labarthe-Hernández, G., 2003. Fissure ignimbrites: fissure-source origin for voluminous ignimbrites of the Sierra Madre Occidental and its relationship with Basin and Range faulting. Geology 31, 773–776.

Aguirre-Díaz, G.J., McDowell, F.W., 1991. The volcanic section at Nazas, Durango, Mexico, and the possibility of widespread Eocene volcanism within the Sierra Madre Occidental. J. Geophys. Res. 96, 13373–13388.

Aguirre-Díaz, G.J., McDowell, F.W., 1993. Nature and timing of faulting and synextensional magmatism in the southern Basin and Range, central-eastern Durango, Mexico. Geol. Soc. Am. Bull. 105, 1435–1444.

Albinson, T., Norman, D.I., Cole, D., Chomiak, B.A., 2001. Controls on formation of low-sulfidation epithermal deposits in Mexico: constraints from fluid inclusion and stable isotope data. Soc. Econ. Geol. Spec. Publ. 8, 1–32.

Armstrong, R.L., Ward, P.L., 1991. Evolving geographic patterns of Cenozoic magmatism in the North American Cordillera: the temporal and spatial association of magmatism and metamorphic core complexes. J. Geophys. Res. 96, 13201–13224.

Best, M.G., Christiansen, E.H., Gromme, S., 2013. Introduction: the 36–18 Ma southern Great Basin, USA, ignimbrite province and flareup: swarms of subduction-related supervolcanoes. Geosphere 9, 260–274.

Bryan, S., 2007. Silicic large igneous provinces. Episodes 30, 1–12.

Bryan, S.E., Ferrari, L., 2013. Large igneous provinces and silicic large igneous provinces: progress in our understanding over the last 25 yr. Geol. Soc. Am. Bull. 125, 1053–1078.

Bryan, S.E., Orozco-Esquivel, T., Ferrari, L., López-Martínez, M., 2013. Pulling apart the mid to late Cenozoic magmatic record of the Gulf of California: is there a Comondú arc?. In: Gomez-Tuena, A., Straub, S.M., Zellmer, G.F. (Eds.), Orogenic Andesites and Crustal Growth, vol. 385. Geological Society of London Special Publication, pp. 389–407.

Busby, C.J., 2012. Extensional and transtensional continental arc basins: case studies from the southwestern U.S. and Mexico. In: Busby, C., Azor, A. (Eds.), Tectonics of Sedimentary Basins: Recent Advances. Wiley-Blackwell, Chichester, West Sussex, UK, pp. 382–404.

Busby, C.J., 2013. Birth of a plate boundary at ca. 12 Ma in the Ancestral Cascades arc, Walker Lane belt of California and Nevada. Geosphere 9, 1147–1160.

Cameron, K.L., Nimz, G.J., Niemeyer, S., Gunn, S., 1989. Southern Cordilleran basaltic andesite suite, southern Chihuahua, Mexico: a link between Tertiary continental arc and flood basalt magmatism in North America. J. Geophys. Res. 94, 7817–7840.

Camprubí, A., Ferrari, L., Cosca, M.A., Cardellach, E., Canals, À., 2003. Ages of epithermal deposits in Mexico: regional significance and links with the evolution of Tertiary volcanism. Econ. Geol. 98, 1029–1037.

Cather, S.M., Dunbar, N.W., McDowell, F.W., McIntosh, W.C., Scholle, P.A., 2009. Climate forcing by iron fertilization from repeated ignimbrite eruptions: the icehouse-silicic large igneous province (SLIP) hypothesis. Geosphere 5, 315–324.

Cochemé, J.J., Demant, A., 1991. Geology of the Yécora area, northern Sierra Madre Occidental, Mexico. In: Pérez-Segura, E., Jacques-Ayala, C. (Eds.), Studies in Sonoran Geology: Geological Society of America Special Paper, vol. 254, pp. 81–94.

Coney, P.J., 1978. Mesozoic–Cenozoic Cordilleran plate tectonics. In: Smith, R.B., Eaton, G.P. (Eds.), Cenozoic Tectonics and Regional Geophysics of the Western Cordillera: Geological Society of America Memoir, vol. 152. Geological Society of America, Boulder, CO, pp. 33–50.

Coney, P.J., Reynolds, S.J., 1977. Cordilleran Benioff zones. Nature 270, 403–406.

Damon, P.E., Shafiqullah, M., Clark, K.F., 1981. Age trends of igneous activity in relation to metallogenesis in the southern Cordillera. Ariz. Geol. Soc. Dig. 14, 137–154.

Dickinson, W.R., Snyder, W.S., 1979. Geometry of subducted slabs related to the San Andreas transform. J. Geol. 87, 609–627.

Dreier, J., 1984. Regional tectonic control of epithermal veins in the Western United States and Mexico. In: Wilkins, J. (Ed.), Gold and Silver Deposits of the Basin and Range Province, Western U.S.A., vol. 15. Arizona Geological Society Digest, pp. 28–50.

Faulds, J.E., Varga, R.J., 1998. The role of accommodation zones and transfer zones in the regional segmentation of extended terranes. In: Faulds, J.E., Stewart, J.H. (Eds.), Accommodation Zones and Transfer Zones: the Regional Segmentation of the Basin and Range Province. Geological Society of America Special Paper, vol. 323, pp. 1–45. Boulder, CO.

Feinstein, M.N., 2007. Contributions to the Geology of the Cuenca de Oro: Chihuahua, Mexico. Department of Geological Sciences. University of Texas at El Paso, El Paso, TX, p. 168.

Ferrari, L., López-Martinez, M., Aguirre-Díaz, G., Carrasco-Núñez, G., 1999. Space–time patterns of Cenozoic arc volcanism in central Mexico: from the Sierra Madre Occidental to the Mexican Volcanic Belt. Geology 27, 303–306.

Ferrari, L., López-Martínez, M., Orozco-Esquivel, T., Bryan, S.E., Duque-Trujillo, J., Lonsdale, P., Solari, L., 2013. Late Oligocene to Middle Miocene rifting and synextensional magmatism in the southwestern Sierra Madre Occidental, Mexico: the beginning of the Gulf of California rift. Geosphere 9, 1161–1200.

Ferrari, L., López-Martínez, M., Rosas-Elguera, J., 2002. Ignimbrite flare-up and deformation in the southern Sierra Madre Occidental, western Mexico: implications for the late subduction history of the Farallon plate. Tectonics 21, 1–24.

Ferrari, L., Valencia-Moreno, M., Bryan, S., 2007. Magmatism and tectonics of the Sierra Madre Occidental and its relation with the evolution of the western margin of North America. In: Alaniz-Álvarez, S.A., Nieto-Samaniego, Á.F. (Eds.), Geology of México: Celebrating the Centenary of the Geological Society of México: Geological Society of America Special Paper, vol. 422, pp. 1–39.

Fink, J.H., Anderson, S.W., 2000. Lava domes and coulees. In: Sigurdsson, H., Houghton, B.F., McNutt, S.R., Rymer, H., Stix, J. (Eds.), Encyclopedia of Volcanoes. Academic Press, San Diego, CA, pp. 307–319.

Fisher, R.V., Schmincke, H.U., 1984. Pyroclastic Rocks. Springer Verlag, Berlin.

Fisher, R.V., Smith, G.A., 1991. Sedimentation in Volcanic Settings: SEPM (Society for Sedimentary Geology) Special Publication No. 45. SEPM (Society for Sedimentary Geology), Tulsa, OK.

Freundt, A., Wilson, C.J.N., Carey, S.N., 2000. Ignimbrites and block-and-ash flow deposits. In: Sigurdsson, H., Houghton, B.F., McNutt, S.R., Rymer, H., Stix, J. (Eds.), Encyclopedia of Volcanoes. Academic Press, San Diego, CA, pp. 581–600.

Galván-Gutiérrez, V.H., 2005. Regional and Local Patterns of Mineralization in the Lower Batopilas and Urique Rivers in Sierra Madre of Chihuahua, Mexico. University of Texas, El Paso, p. 115.

Gans, P.B., 1997. Large-magnitude Oligo-Miocene extension in southern Sonora: implications for the tectonic evolution of northwest Mexico. Tectonics 16, 388–408.

Gans, P.B., Blair, K.D., MacMillan, I., Wong, M.S., Roldán-Quintana, J., 2003. Structural and magmatic evolution of the Sonoran rifted margin: a preliminary report. Geol. Soc. Am. Abstr. Progr. 35, 21.

González-León, C.M., McIntosh, W.C., Lozano-Santacruz, R., Valencia-Moreno, M., Amaya-Martínez, R., Rodríguez-Castañeda, J.L., 2000. Cretaceous and Tertiary sedimentary, magmatic, and tectonic evolution of north-central Sonora (Arizpe and Bacanuchi Quadrangles), northwest Mexico. Geol. Soc. Am. Bull. 112, 600–610.

Goodell, P.C., 1995. Porphyry copper deposits along the Batopilas lineament, Chihuahua, Mexico. In: Pierce, F.W., Bolm, J.G. (Eds.), Porphyry Copper Deposits of the American Cordillera: Arizona Geological Society Digest, vol. 20, p. 544.

Grijalva-Noriega, F.J., Roldán-Quintana, J., 1998. An overview of the Cenozoic tectonic and magmatic evolution of Sonora, northwestern Mexico. Rev. Mex. Cienc. 15, 145–156.

Gustin, M.M., 2011. Technical Report on the San Miguel Project, Guazapares Mining District, Chihuahua, Mexico. Prepared for Paramount Gold and Silver Corp. Mine Development Associates, Reno, NV.

Gustin, M.M., 2012. Updated Technical Report on the San Miguel Project Gold and Silver Resources, Guazapares Mining District, Chihuahua, Mexico, Prepared for Paramount Gold and Silver Corp. Mine Development Associates, Reno, NV.

Henry, C., Aranda-Gómez, J.J., 2000. Plate interactions control middle-late Miocene, proto-Gulf and Basin and Range extension in the southern Basin and Range. Tectonophysics 218, 1–26.

Henry, C.D., McIntosh, W., McDowell, F.W., Lipman, P.W., Chapin, C.E., Richardson, M.T., 2010. Distribution, timing, and controls of the mid-Cenozoic

ignimbrite flareup in western North America. Geol. Soc. Am. Abstr. Progr. 42, 144.
Jerram, D., Petford, N., 2011. The Field Description of Igneous Rocks, second ed. Wiley-Blackwell, Chichester, UK.
Lipman, P.W., 2007. Incremental assembly and prolonged consolidation of Cordilleran magma chambers: evidence from the Southern Rocky Mountain volcanic field. Geosphere 3, 42–70.
McDowell, F.W., 2007. Geologic Transect across the Northern Sierra Madre Occidental Volcanic Field, Chihuahua and Sonora, Mexico. In: Geological Society of America Digital Map and Chart Series, vol. 6.
McDowell, F.W., Clabaugh, S.E., 1979. Ignimbrites of the Sierra Madre Occidental and their relation to the tectonic history of western Mexico. In: Chapin, C.E., Elston, W.E. (Eds.), Ash-Flow Tuffs: Geological Society of America Special Paper, vol. 180, pp. 113–124.
McDowell, F.W., Keizer, R.P., 1977. Timing of mid-Tertiary volcanism in the Sierra Madre Occidental between Durango City and Mazatlan, Mexico. Geol. Soc. Am. Bull. 88, 1479–1487.
McDowell, F.W., Mauger, R.L., 1994. K–Ar and U–Pb zircon chronology of Late Cretaceous and Tertiary magmatism in central Chihuahua State, Mexico. Geol. Soc. Am. Bull. 106, 118–132.
McDowell, F.W., McIntosh, W.C., 2012. Timing of intense magmatic episodes in the northern and central Sierra Madre Occidental, western Mexico. Geosphere 8, 1502–1526.
McDowell, F.W., Roldán-Quintana, J., Amaya-Martínez, R., 1997. Interrelationship of sedimentary and volcanic deposits associated with Tertiary extension in Sonora, Mexico. Geol. Soc. Am. Bull. 109, 1349–1360.
McDowell, F.W., Roldán-Quintana, J., Connelly, J.N., 2001. Duration of Late Cretaceous–early Tertiary magmatism in east-central Sonora, Mexico. Geol. Soc. Am. Bull. 113, 521–531.
Minjárez-Sosa, I., Montaño-Jiménez, T.R., Ochoa-Granillo, J.A., Grijalva-Noriega, F.J., Ochoa-Landín, L.H., Herrera-Urbina, S., Guzmán-Espinosa, J.B., Mancilla-Gutiérrez, A.A., 2002. Carta Geológico-Minera Ciudad Obregón G12-3 Sonora, Chihuahua y Sinaloa. Servicio Geológico Mexicano.
Murray, B.P., Busby, C.J., Ferrari, L., Solari, L.A., 2013. Synvolcanic crustal extension during the mid-Cenozoic ignimbrite flare-up in the northern Sierra Madre Occidental, Mexico: evidence from the Guazapares Mining District region, western Chihuahua. Geosphere 9, 1201–1235.
Nieto-Samaniego, Á.F., Ferrari, L., Alaniz-Álvarez, S.A., Labarthe-Hernández, G., Rosas-Elguera, J., 1999. Variation of Cenozoic extension and volcanism across the southern Sierra Madre Occidental volcanic province, Mexico. Geol. Soc. Am. Bull. 111, 347–363.
Price, J.G., Conlon, S.T., Henry, C.D., 1988. Tectonic Controls on Orientation and Size of Epithermal Veins. Univ. Mo., Rolla, MO.
Ramírez-Tello, E., García-Peralta, Á.A., 2004. Carta Geológico-Minera Témoris G12–B39 Chihuahua. Servicio Geológico Mexicano.
Randall, R.,J.A., Saldana, A.,E., Clark, K.F., 1994. Exploration in a volcano-plutonic center at Guanajuato, Mexico. Econ. Geol. 89, 1722–1751.
Roy, D., Trinder, I.D., Lustig, G., 2008. Report on the San Miguel Project, Guazapares Mining District, Chihuahua, Mexico for Paramount Gold and Silver Corp. A.C.A. Howe International Limited, Toronto, Ontario.
Scheubel, F.R., Clark, K.F., Porter, E.W., 1988. Geology, tectonic environment, and structural controls in the San Martín de Bolaños district, Jalisco, Mexico. Econ. Geol. 83, 1703–1720.
Sellepack, S.M., 1997. The Geology and Geochemistry of the El Sauzal Gold Prospect, Southwest Chihuahua, Mexico. Department of Geological Sciences. University of Texas at El Paso, El Paso, TX, p. 118.
Sigurdsson, H., Houghton, B.F., McNutt, S.R., Rymer, H., Stix, J., 2000. Encyclopedia of Volcanoes. Academic Press, San Diego, California.
Staude, J.G., Barton, M.D., 2001. Jurassic to Holocene tectonics, magmatism, and metallogeny of northwestern Mexico. Geol. Soc. Am. Bull. 113, 1357–1374.
Ward, P.L., 1991. On plate tectonics and the geologic evolution of southwestern North America. J. Geophys. Res. 96, 12479–12496.
Wark, D.A., 1991. Oligocene ash flow volcanism, northern Sierra Madre Occidental: role of mafic and intermediate-composition magmas in rhyolite genesis. J. Geophys. Res. 96, 13389–13411.
Wark, D.A., Kempter, K.A., McDowell, F.W., 1990. Evolution of waning subduction-related magmatism, northern Sierra Madre Occidental, Mexico. Geol. Soc. Am. Bull. 102, 1555–1564.
Wilkerson, G., Deng, Q., Llavona, R., Goodell, P., 1988. Batopilas Mining District, Chihuahua, Mexico. Econ. Geol. 83, 1721–1736.
Wong, M.S., Gans, P.B., Scheier, J., 2010. The $^{40}Ar/^{39}Ar$ thermochronology of core complexes and other basement rocks in Sonora, Mexico: implications for Cenozoic tectonic evolution of northwestern Mexico. J. Geophys. Res. 115.
Wood, D.R., Durgin, D.C., 2009. Technical Report Project Update: San Miguel Project, Chihuahua, Mexico. Prepared for Paramount Gold and Silver Corp. Delve Consultants, L.L.C., Sparks, Nevada.